Chapter 11

FREQUENCY DOMAIN PROPERTIES OF MULTILINEAR INTERVAL SYSTEMS

In this chapter we continue our development of the theory of robustness under multilinear interval uncertainty. We consider the robust Hurwitz stability and performance of control systems which contain transfer functions that are ratios of multilinear interval polynomials. The characteristic polynomial of such a system is a multilinear interval polynomial. We extend the Generalized Kharitonov Theorem (Chapter 7) to this case. This extension provides a set of extremal manifolds which serve as a reduced test set for robust stability. These manifolds are the multilinear counterpart of the extremal segments derived for the linear case and possess the same optimality and boundary generating properties. In particular, they can be used, in conjunction with the polytopic approximation based on the Mapping Theorem derived in Chapter 10, to generate frequency domain templates, Bode and Nyquist envelopes, to calculate worst case stability margins and to determine the robust performance of control systems under mixed parametric/unstructured uncertainty in a computationally efficient manner.

11.1 INTRODUCTION

Consider the feedback configuration shown in Figure 11.1. $F(s)$ is a fixed controller and $G_1(s)$ and $G_2(s)$ are independent subsystems containing parameter uncertainty. Let

$$F(s) := \frac{F_1(s)}{F_2(s)}, \quad G_1(s) := \frac{P_{11}(s)}{P_{21}(s)}, \quad G_2(s) := \frac{P_{12}(s)}{P_{22}(s)}. \tag{11.1}$$

If the subsystems $G_1(s)$ and $G_2(s)$ contain independent parameters it is reasonable to model them as *interval* or *linear interval* systems $\mathbf{G}_i(s)$, $i = 1, 2$. The

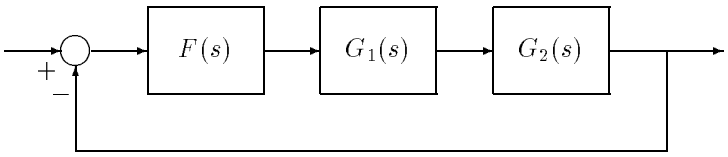

Figure 11.1. Interconnected Feedback System

characteristic polynomial of this feedback system is:

$$\delta(s) := F_1(s)P_{11}(s)P_{12}(s) + F_2(s)P_{21}(s)P_{22}(s). \tag{11.2}$$

The open loop transfer function

$$T^o(s) = F(s)G_1(s)G_2(s) = \frac{F_1(s)P_{11}(s)P_{12}(s)}{F_2(s)P_{21}(s)P_{22}(s)}$$

and the closed loop transfer function

$$\begin{aligned} T^c(s) &= \frac{F(s)G_1(s)G_2(s)}{1 + F(s)G_1(s)G_2(s)} \\ &= \frac{F_1(s)P_{11}(s)P_{12}(s)}{F_1(s)P_{11}(s)P_{12}(s) + F_2(s)P_{21}(s)P_{22}(s)}. \end{aligned}$$

These transfer functions have numerator and denominator polynomials that are multilinear functions of interval polynomials. In addition, the numerator and denominator in $T^o(s)$ have independent interval polynomials (parameters), but in $T^c(s)$ the numerator and denominator contain *common* interval polynomials.

For this class of systems we are interested in the following types of questions:

1) Does $F(s)$ robustly stabilize the system or not?

2) If $F(s)$ does robustly stabilize the system, what are the worst case gain margin, phase margin, parametric stability margin, H_∞ stability margin and performance measured in terms of H_∞ norms, as the parameters range over the uncertainty set?

3) How can one construct the Bode magnitude and phase, and Nyquist plots of various transfer function sets such as $T^o(s)$ and $T^c(s)$ generated by the uncertain parameters?

These questions were addressed in the previous chapter for an arbitrary stability region using the Mapping Theorem as a computational tool. In this chapter, we focus on the case of Hurwitz stability and show how the Generalized Kharitonov Theorem (GKT) derived in Chapter 7 can be extended to this multilinear case to

provide a great deal of simplification and computational efficiency. We first derive a multilinear version of GKT. This generalization provides us with an extremal test set for multilinear interval systems, with drastically reduced dimension of the parameter space, from which all the above questions can be answered. It will tell us, essentially that as long as the dependencies are multilinear, worst case stability margins and performance can be calculated for an arbitrary control system containing interval subsystems by replacing each interval subsystem $\mathbf{G}^i(s)$ by the corresponding extremal set of systems $\mathbf{G}^i_{\mathrm{E}}(s)$. The polytopic approximation derived in the last chapter can then be used on this extremal set to give a highly efficient computational solution to the design and analysis questions posed above. In the next section we describe the extension of GKT to the multilinear case.

11.2 MULTILINEAR INTERVAL POLYNOMIALS

To avoid notational complexity, we first consider the simplest multilinear polynomial form motivated by (11.2). We consider the Hurwitz stability of the characteristic polynomial family of the form

$$\delta(s) := F_1(s)P_{11}(s)P_{12}(s) + F_2(s)P_{21}(s)P_{22}(s) \tag{11.3}$$

where $F_i(s)$ are fixed real polynomials and $P_{ij}(s)$ are real interval polynomials with *independently* varying parameters. Let $\mathbf{p}$ denote the ordered set of coefficients of the polynomials $\{P_{11}(s), P_{12}(s)P_{21},(s)P_{22}(s)\}$. We assume that each coefficient varies in an independent interval, or equivalently that $\mathbf{p}$ varies in an axis-parallel box $\mathbf{\Pi}$. The dimension of the parameter space here is equal to the number of independently varying parameters contained in these polynomials. Referring to the notation used in Chapter 7 we let $\mathbf{P}_{ij}(s)$ denote the interval polynomial family and $\mathcal{K}_{ij}(s)$ and $\mathcal{S}_{ij}(s)$ denote the respective Kharitonov polynomials and Kharitonov segments (refer to Chapter 7 for the definition of these segments). The family of uncertain polynomials is represented, using the notation of Chapter 7, as

$$\mathbf{\Delta}(s) := F_1(s)\mathbf{P}_{11}(s)\mathbf{P}_{12}(s) + F_1(s)\mathbf{P}_{21}(s)\mathbf{P}_{22}(s). \tag{11.4}$$

Define

$$\mathbf{\Delta}^1_{\mathrm{E}}(s) := F_1(s)\mathcal{S}_{11}(s)\mathcal{S}_{12}(s) + F_2(s)\mathcal{K}_{21}(s)\mathcal{K}_{22}(s)$$
$$\mathbf{\Delta}^2_{\mathrm{E}}(s) := F_1(s)\mathcal{K}_{11}(s)\mathcal{K}_{12}(s) + F_2(s)\mathcal{S}_{21}(s)\mathcal{S}_{22}(s)$$

and introduce the extremal manifolds

$$\mathbf{\Delta}_{\mathrm{E}}(s) := \mathbf{\Delta}^1_{\mathrm{E}}(s) \cup \mathbf{\Delta}^2_{\mathrm{E}}(s). \tag{11.5}$$

Lemma 11.1 *Under the assumption that every polynomial in $\mathbf{\Delta}(s)$ is of the same degree and the parameters (coefficients) in the interval polynomials $\mathbf{P}_{11}(s)$, $\mathbf{P}_{12}(s)$, $\mathbf{P}_{21}(s)$, $\mathbf{P}_{22}(s)$ are independent, $\mathbf{\Delta}(s)$ is Hurwitz stable if and only if $\mathbf{\Delta}_{\mathrm{E}}(s)$ is Hurwitz stable.*

Proof. The proof consists of recursive application of the Generalized Kharitonov Theorem (GKT) in Chapter 7. From GKT, $\mathbf{\Delta}(s)$ is stable if and only if the following families:

$$F_1(s)\mathcal{S}_{11}(s)P_{12}(s) + F_2(s)\mathcal{K}_{21}(s)P_{22}(s) \tag{11.6}$$

and

$$F_1(s)\mathcal{K}_{11}(s)P_{12}(s) + F_2(s)\mathcal{S}_{21}(s)P_{22}(s) \tag{11.7}$$

are stable for each polynomial $P_{12}(s) \in \mathbf{P}_{12}(s)$ and $P_{22}(s) \in \mathbf{P}_{22}(s)$. Since each expression in (11.6) and (11.7) is linear in $P_{12}(s)$ and $P_{22}(s)$, we can apply GKT again to each such family and conclude that the stability of the family (11.6) is equivalent to the stability of the families of polynomials

$$F_1(s)\mathcal{S}_{11}(s)\mathcal{S}_{12}(s) + F_2(s)\mathcal{K}_{21}(s)\mathcal{K}_{22}(s) \tag{11.8}$$

$$F_1(s)\mathcal{S}_{11}(s)\mathcal{K}_{12}(s) + F_2(s)\mathcal{K}_{21}(s)\mathcal{S}_{22}(s) \tag{11.9}$$

and the stability of the family (11.7) is equivalent to the stability of the families

$$F_1(s)\mathcal{K}_{11}(s)\mathcal{K}_{12}(s) + F_2(s)\mathcal{S}_{21}(s)\mathcal{S}_{22}(s) \tag{11.10}$$

$$F_1(s)\mathcal{K}_{11}(s)\mathcal{S}_{12}(s) + F_2(s)\mathcal{S}_{21}(s)\mathcal{K}_{22}(s). \tag{11.11}$$

We note that each element of the families of polynomials in (11.9) and (11.11) is a polytope of polynomials. Therefore, by the Edge Theorem in Chapter 6, the stability of each such polytope is equivalent to the stability of its exposed edges. Since the segment polynomials are convex combinations of Kharitonov polynomials, we see that these exposed edges are contained in the families (11.8) and (11.10). Therefore, the theorem holds. ♣

For the general case, we have the *multilinear interval polynomial*

$$\mathbf{\Delta}(s) = F_1(s)\mathbf{P}_{11}(s)\cdots\mathbf{P}_{1r_1}(s) + \cdots + F_m(s)\mathbf{P}_{m1}(s)\cdots\mathbf{P}_{mr_m}(s) \tag{11.12}$$

where $F_i(s)$ are fixed and $P_{ij}(s)$ are interval polynomial families. The arguments used in the earlier case carry over to this case and the result will be presented without repeating the proof. We define

$$\begin{aligned}\mathbf{\Delta}^l_{\mathrm{E}}(s) := {} & F_1(s)\mathcal{K}_{11}(s)\cdots\mathcal{K}_{1r_1}(s) + \cdots + F_{l-1}(s)\mathcal{K}_{l-1,1}(s)\cdots\mathcal{K}_{l-1,r_{l-1}}(s) \\ & + F_l(s)\mathcal{S}_{l,1}(s)\cdots\mathcal{S}_{l,r_l}(s) + F_{l+1}\mathcal{K}_{l+1,1}(s)\cdots\mathcal{K}_{l+1,r_{l+1}} \\ & + \cdots + F_m(s)\mathcal{K}_{m,1}(s)\cdots\mathcal{K}_{m,r_m}(s)\end{aligned} \tag{11.13}$$

and introduce the *extremal manifolds*

$$\mathbf{\Delta}_{\mathrm{E}}(s) := \cup_{l=1}^{m}\mathbf{\Delta}^l_{\mathrm{E}}(s). \tag{11.14}$$

Theorem 11.1 *Under the assumption that every polynomial in $\mathbf{\Delta}(s)$ is of the same degree and the parameters (coefficients) in the interval polynomials $\mathbf{P}_{ij}(s)$ are independent, $\mathbf{\Delta}(s)$ is Hurwitz stable if and only if $\mathbf{\Delta}_{\mathrm{E}}(s)$ is Hurwitz stable.*

Remark 11.1. The theorem is also valid when some of the polynomials $F_i(s)$ are complex or quasipolynomials This follows from the corresponding fact that GKT (Chapter 7) holds when some of the fixed polynomials $F_i(s)$ are replaced by complex polynomials or quasipolynomials.

The next example illustrates the construction of the set of manifolds.

Example 11.1. (Extremal Manifolds for Multilinear Systems) Consider the characteristic polynomial

$$\delta(s) = F_1(s)P_{11}(s)P_{12}(s) + F_2(s)P_{21}(s)P_{22}(s)$$

where the fixed polynomials $F_1(s)$ are

$$F_1(s) = s + f_1, \qquad F_2(s) = s + f_2$$

and the interval polynomials are

$$\begin{aligned} P_{11}(s) &= a_2 s^2 + a_1 s + a_0, & P_{12}(s) &= b_2 s^2 + b_1 s + b_0, \\ P_{21}(s) &= c_2 s^2 + c_1 s + c_0, & P_{22}(s) &= d_2 s^2 + d_1 s + d_0, \end{aligned}$$

with all coefficients varying independently. The Kharitonov polynomials corresponding to $P_{11}(s)$, $P_{12}(s)$, $P_{21}(s)$ and $P_{22}(s)$ are:

$$\begin{aligned} K^1_{P_{11}}(s) &= a_2^+ s^2 + a_1^- s + a_0^-, & K^2_{P_{11}}(s) &= a_2^+ s^2 + a_1^+ s + a_0^-, \\ K^3_{P_{11}}(s) &= a_2^- s^2 + a_1^- s + a_0^+, & K^4_{P_{11}}(s) &= a_2^- s^2 + a_1^+ s + a_0^+, \\ K^1_{P_{12}}(s) &= b_2^+ s^2 + b_1^- s + b_0^-, & K^2_{P_{12}}(s) &= b_2^+ s^2 + b_1^+ s + b_0^-, \\ K^3_{P_{12}}(s) &= b_2^- s^2 + b_1^- s + b_0^+, & K^4_{P_{12}}(s) &= b_2^- s^2 + b_1^+ s + b_0^+, \\ K^1_{P_{21}}(s) &= c_2^+ s^2 + c_1^- s + c_0^-, & K^2_{P_{21}}(s) &= c_2^+ s^2 + c_1^+ s + c_0^-, \\ K^3_{P_{21}}(s) &= c_2^- s^2 + c_1^- s + a_0^+, & K^4_{P_{21}}(s) &= c_2^- s^2 + c_1^+ s + c_0^+, \\ K^1_{P_{22}}(s) &= d_2^+ s^2 + d_1^- s + d_0^-, & K^2_{P_{22}}(s) &= d_2^+ s^2 + d_1^+ s + d_0^-, \\ K^3_{P_{22}}(s) &= d_2^- s^2 + d_1^- s + d_0^+, & K^4_{P_{22}}(s) &= d_2^- s^2 + d_1^+ s + d_0^+. \end{aligned}$$

The sets of segments joining appropriate pairs of Kharitonov polynomials can also be obtained. Here we give only the segments corresponding to the interval polynomial $P_{11}(s)$; others can be similarly obtained.

$$\begin{aligned} S^1_{P_{11}}(s) &= \lambda K^1_{P_{11}}(s) + (1-\lambda) K^2_{P_{11}}(s) \\ S^2_{P_{11}}(s) &= \lambda K^1_{P_{11}}(s) + (1-\lambda) K^3_{P_{11}}(s) \\ S^3_{P_{11}}(s) &= \lambda K^2_{P_{11}}(s) + (1-\lambda) K^4_{P_{11}}(s) \\ S^4_{P_{11}}(s) &= \lambda K^3_{P_{11}}(s) + (1-\lambda) K^4_{P_{11}}(s). \end{aligned}$$

From the above, we now can write the manifolds:

$$\mathbf{\Delta}_1(s) = \left\{ F_1(s)K^i_{P_{11}}(s)K^j_{P_{12}}(s) + F_2(s)S^k_{P_{21}}(s)S^l_{P_{22}}(s) : (i,j,k,l) \in \underline{4} \times \underline{4} \times \underline{4} \times \underline{4} \right\}$$
$$\mathbf{\Delta}_2(s) = \left\{ F_1(s)S^i_{P_{11}}(s)S^j_{P_{12}}(s) + F_2(s)K^k_{P_{21}}(s)K^l_{P_{22}}(s) : (i,j,k,l) \in \underline{4} \times \underline{4} \times \underline{4} \times \underline{4} \right\}$$

and

$$\mathbf{\Delta}_{\mathrm{E}}(s) = \mathbf{\Delta}_1 \cup \mathbf{\Delta}_2.$$

As we can see, the total parameter space is of dimension 12. However, our problem is now reduced to checking the stability of 512 two-dimensional manifolds. Notice that each manifold remains of dimension two, even though the dimension of the parameter space can be increased arbitrarily. The dimension of the manifolds is increased only if the number of interval polynomials in a product term is increased.

11.2.1 Dependencies Between the Perturbations

The theorem is stated assuming that the polynomials $P_{ij}(s)$ perturb independently. In an interconnected multiloop control system, it will in general happen that some of the polynomials $P_{ij}(s)$ are in fact identical (see, for example, Exercise 11.1). Such dependencies can be easily handled. To avoid introducing cumbersome notation we illustrate the procedure with an example.

Consider the following multilinear interval polynomial family with dependencies between the perturbations:

$$\delta(s,\mathbf{p}) := F_1(s)P_{11}(s)P_{12}(s) + F_2(s)P_{21}(s)P_{22}(s) + F_3(s)P_{31}(s)P_{32}(s)$$

where $P_{11}(s) = P_{21}(s)$ and $P_{22}(s) = P_{32}(s)$ and each polynomial $P_{ij}(s)$ is interval. If we rewrite embedding the above constraints, we have

$$\delta(s,\mathbf{p}) = F_1(s)P_{11}(s)P_{12}(s) + F_2(s)P_{11}(s)P_{22}(s) + F_3(s)P_{31}(s)P_{22}(s). \qquad (11.15)$$

Let us first fix $P_{11}(s)$ and $P_{31}(s)$ and apply GKT. This tells us that the Hurwitz stability of the set $\mathbf{\Delta}(s)$ is equivalent to stability of the sets

$$\mathbf{I}_1(s) = \{F_1(s)P_{11}(s)\mathcal{S}_{12}(s) + (F_2(s)P_{11}(s) + F_3(s)P_{31}(s))\mathcal{K}_{22}(s)\}$$
$$\mathbf{I}_2(s) = \{F_1(s)P_{11}(s)\mathcal{K}_{12}(s) + (F_2(s)P_{11}(s) + F_3(s)P_{31}(s))\mathcal{S}_{22}(s)\}$$

for each $(P_{11}(s), P_{31}(s)) \in \mathbf{P}_{11}(s) \times \mathbf{P}_{31}(s)$. We now apply GKT again to each of the sets $\mathbf{I}_1(s)$ and $\mathbf{I}_2(s)$ letting $P_{11}(s)$ and $P_{31}(s)$ now vary. This leads to the condition that the robust stability of $\mathbf{\Delta}(s)$ is equivalent to robust stability of the manifolds:

$$\mathbf{\Delta}_1(s) = \{\delta(s,\mathbf{p}) : P_{11} \in \mathcal{S}_{11},\ P_{12} \in \mathcal{S}_{12},\ P_{22} \in \mathcal{K}_{22},\ P_{31} \in \mathcal{K}_{31}\}$$
$$\mathbf{\Delta}_2(s) = \{\delta(s,\mathbf{p}) : P_{11} \in \mathcal{S}_{11},\ P_{12} \in \mathcal{K}_{12},\ P_{22} \in \mathcal{S}_{22},\ P_{31} \in \mathcal{K}_{31}\}$$
$$\mathbf{\Delta}_3(s) = \{\delta(s,\mathbf{p}) : P_{11} \in \mathcal{K}_{11},\ P_{12} \in \mathcal{S}_{12},\ P_{22} \in \mathcal{K}_{22},\ P_{31} \in \mathcal{S}_{31}\}$$
$$\mathbf{\Delta}_4(s) = \{\delta(s,\mathbf{p}) : P_{11} \in \mathcal{K}_{11},\ P_{12} \in \mathcal{K}_{12},\ P_{22} \in \mathcal{S}_{22},\ P_{31} \in \mathcal{S}_{31}\}.$$

Since $\mathbf{\Delta}_3(s)$ is a polytope, we now can apply the Edge Theorem (Chapter 6) to conclude that this is stable if and only if its exposed edges are. These exposed edges are

$$\{\delta(s,\mathbf{p}) : P_{11} \in \mathcal{K}_{11},\ P_{12} \in \mathcal{S}_{12},\ P_{22} \in \mathcal{K}_{22},\ P_{31} \in \mathcal{K}_{31}\} \tag{11.16}$$

$$\{\delta(s,\mathbf{p}) : P_{11} \in \mathcal{K}_{11},\ P_{12} \in \mathcal{K}_{12},\ P_{22} \in \mathcal{K}_{22},\ P_{31} \in \mathcal{S}_{31}\}. \tag{11.17}$$

It is easy to see that the manifolds (11.16) and (11.17) are contained in $\mathbf{\Delta}_1(s)$ and $\mathbf{\Delta}_4(s)$ respectively. Therefore the set of manifolds that finally need to be checked is

$$\mathbf{\Delta}_{\mathrm{E}}(s) := \mathbf{\Delta}_1(s) \cup \mathbf{\Delta}_2(s) \cup \mathbf{\Delta}_4(s). \tag{11.18}$$

Interval Polynomial Matrix

An important special case of dependent perturbations is that of interval polynomial matrices. Let $M(s)$ be an $n \times n$ polynomial matrix whose ij^{th} entry is the polynomial $P_{ij}(s)$. The characteristic polynomial associated with this matrix is $\det[M(s)]$. We assume that each $P_{ij}(s)$ belongs to an interval family $\mathbf{P}_{ij}(s)$ and the parameters of each $P_{ij}(s)$ are independent of all others. Let $\mathbf{M}(s)$ denote the corresponding set of matrices. We will say that the set is stable if $\det[M(s)]$ is Hurwitz stable for every $M(s) \in \mathbf{M}(s)$. To test Hurwitz stability of the family of characteristic polynomials so obtained we have the following result. Let $\mathbf{T}$ be the set of $n \times n$ permutation matrices obtained from the identity matrix. Corresponding to each $T \in \mathbf{T}$, introduce the set of polynomial matrices $M_T(s)$ where $P_{ij}(s)$ ranges over $\mathcal{K}_{ij}(s)$ if the ij^{th} entry of T is 0 and $P_{ij}(s)$ ranges over $\mathcal{S}_{ij}(s)$ if the ij^{th} entry of T is 1. Let $\mathbf{M}^*(s)$ denote the collection of matrices $M_T(s)$ obtained by letting T range over all permutation matrices $\mathbf{T}$.

Theorem 11.2 *$\mathbf{M}(s)$ is Hurwitz stable if and only if $\mathbf{M}^*(s)$ is Hurwitz stable.*

Proof. Consider the case $n = 3$.

$$M(s) := \begin{bmatrix} P_{11}(s) & P_{12}(s) & P_{13}(s) \\ P_{21}(s) & P_{22}(s) & P_{23}(s) \\ P_{31}(s) & P_{32}(s) & P_{33}(s) \end{bmatrix}.$$

Then

$$\begin{aligned} \det[M(s)] \ :=\ & P_{11}(s)P_{22}(s)P_{33}(s) + P_{12}(s)P_{23}(s)P_{31}(s) + P_{21}(s)P_{32}(s)P_{13}(s) \\ & - P_{13}(s)P_{22}(s)P_{31}(s) - P_{12}(s)P_{21}(s)P_{33}(s) - P_{11}(s)P_{23}(s)P_{32}(s). \end{aligned}$$

We see that we have a multilinear interval polynomial with dependencies. We can apply GKT recursively as we did in the previous example. We omit the detailed derivation. The final result is that the following six sets of manifolds need to be checked in order to determine the stability of the set:

$$\mathbf{\Delta}_1(s) := \{\det[M(s)] : P_{11} \in \mathcal{S}_{11},\ P_{22} \in \mathcal{S}_{22},\ P_{33} \in \mathcal{S}_{33},\ P_{12} \in \mathcal{K}_{12},$$

$$
\begin{aligned}
&P_{23} \in \mathcal{K}_{23},\ P_{31} \in \mathcal{K}_{31},\ P_{21} \in \mathcal{K}_{21},\ P_{32} \in \mathcal{K}_{32},\ P_{13} \in \mathcal{K}_{13}\} \\
\mathbf{\Delta}_2(s) := \{\det[M(s)] : &P_{11} \in \mathcal{S}_{11},\ P_{22} \in \mathcal{K}_{22},\ P_{33} \in \mathcal{K}_{33},\ P_{12} \in \mathcal{K}_{12}, \\
&P_{23} \in \mathcal{S}_{23},\ P_{31} \in \mathcal{K}_{31},\ P_{21} \in \mathcal{K}_{21},\ P_{32} \in \mathcal{S}_{32},\ P_{13} \in \mathcal{K}_{13}\} \\
\mathbf{\Delta}_3(s) := \{\det[M(s)] : &P_{11} \in \mathcal{K}_{11},\ P_{22} \in \mathcal{K}_{22},\ P_{33} \in \mathcal{S}_{33},\ P_{12} \in \mathcal{S}_{12}, \\
&P_{23} \in \mathcal{K}_{23},\ P_{31} \in \mathcal{K}_{31},\ P_{21} \in \mathcal{S}_{21},\ P_{32} \in \mathcal{K}_{32},\ P_{13} \in \mathcal{K}_{13}\} \\
\mathbf{\Delta}_4(s) := \{\det[M(s)] : &P_{11} \in \mathcal{K}_{11},\ P_{22} \in \mathcal{S}_{22},\ P_{33} \in \mathcal{K}_{33},\ P_{12} \in \mathcal{K}_{12}, \\
&P_{23} \in \mathcal{K}_{23},\ P_{31} \in \mathcal{S}_{31},\ P_{21} \in \mathcal{K}_{21}, P_{32} \in \mathcal{K}_{32},\ P_{13} \in \mathcal{S}_{13}\} \\
\mathbf{\Delta}_5(s) := \{\det[M(s)] : &P_{11} \in \mathcal{K}_{11},\ P_{22} \in \mathcal{K}_{22},\ P_{33} \in \mathcal{K}_{33},\ P_{12} \in \mathcal{K}_{12}, \\
&P_{23} \in \mathcal{K}_{23},\ P_{31} \in \mathcal{K}_{31},\ P_{21} \in \mathcal{S}_{21},\ P_{32} \in \mathcal{S}_{32},\ P_{13} \in \mathcal{S}_{13}\} \\
\mathbf{\Delta}_6(s) := \{\det[M(s)] : &P_{11} \in \mathcal{K}_{11},\ P_{22} \in \mathcal{K}_{22},\ P_{33} \in \mathcal{K}_{33},\ P_{12} \in \mathcal{S}_{12}, \\
&P_{23} \in \mathcal{S}_{23},\ P_{31} \in \mathcal{S}_{31},\ P_{21} \in \mathcal{K}_{21},\ P_{32} \in \mathcal{K}_{32},\ P_{13} \in \mathcal{K}_{13}\}\,.
\end{aligned}
$$

The reader can verify that the above expressions for the characteristic polynomials correspond to the family $\mathbf{M}^*(s)$ in this case. The result for arbitrary n is proved similarly. ♣

Boundary Generating Property of the Extremal Manifolds

We have established that Hurwitz stability of the family $\mathbf{\Delta}(s)$ is equivalent to the stability of the manifolds $\mathbf{\Delta}_{\mathrm{E}}(s)$. This equivalence also follows from the following boundary result relating the image sets $\mathbf{\Delta}(j\omega)$ and $\mathbf{\Delta}_{\mathrm{E}}(j\omega)$.

Theorem 11.3

$$
\partial\mathbf{\Delta}(j\omega) \subset \mathbf{\Delta}_{\mathrm{E}}(j\omega) \tag{11.19}
$$

Proof. The set $\mathbf{\Delta}(s)$ is a multilinear function of interval polynomials $\mathbf{P}_{ij}(s)$. The boundaries of the sum and product of two complex plane sets $\mathcal{Z}_i$ and $\mathcal{Z}_j$ $(i \neq j)$ satisfy the following properties:

$$
\begin{aligned}
\partial(\mathcal{Z}_i + \mathcal{Z}_j) &\subseteq \partial\mathcal{Z}_i + \partial\mathcal{Z}_j \\
\partial(\mathcal{Z}_i \cdot \mathcal{Z}_j) &\subseteq \partial\mathcal{Z}_i \cdot \partial\mathcal{Z}_j\,.
\end{aligned}
$$

Therefore, the boundary of $\mathbf{\Delta}(j\omega)$ is obtained by replacing each set $\mathbf{P}_{ij}(j\omega)$ with its boundary. However $\mathbf{P}_{ij}(j\omega)$ is an axis parallel rectangle whose vertices are the $j\omega$ images of the Kharitonov polynomials and whose edges are the $j\omega$ images of the Kharitonov segments. Equation (11.19) follows from this. ♣

The boundary result established above implies that the problem of checking robust stability is now reduced to verifying that the origin is excluded from the set $\mathbf{\Delta}_{\mathrm{E}}(j\omega)$ for each ω in $[0, \infty)$. This is a great deal simpler than the original problem because of the greatly reduced dimensionality of the set $\mathbf{\Delta}_{\mathrm{E}}(s)$ relative to the original set $\mathbf{\Delta}(s)$. However, this verification is still not easy because the set $\mathbf{\Delta}_{\mathrm{E}}(s)$ is multilinear in the parameters λ_i. At this point, the Mapping Theorem can be brought in and

used to approximate $\mathbf{\Delta}_{\mathrm{E}}(j\omega)$. Indeed, since $\mathbf{\Delta}_{\mathrm{E}}(s)$ depends multilinearly on the parameters λ_{ij} associated with the Kharitonov segments, the vertex set of $\mathbf{\Delta}(s)$ can be generated by setting the $P_{ij}(s)$ to the corresponding Kharitonov polynomials. Let

$$\mathbf{\Delta}_{\mathrm{K}}(s) = \{\delta(s,\mathbf{p}) \ : \ P_{ij}(s) = K_{ij}^{i_{ij}}(s), \quad i_{ij} \in \underline{4}, \quad i \in \underline{m}, \quad j \in \underline{r_m}\}. \tag{11.20}$$

We can also introduce the polytopic set consisting of convex combinations of the vertex polynomials:

$$\bar{\mathbf{\Delta}}(s) = \{\lambda v_i(s) + (1-\lambda)v_j(s) \ : \ v_i(s), v_j(s) \in \mathbf{\Delta}_{\mathrm{K}}(s), \quad \lambda \in [0,1]\}. \tag{11.21}$$

It follows from the Mapping Theorem now, that

$$co\ \mathbf{\Delta}_{\mathrm{E}}(j\omega) = co\ \mathbf{\Delta}_{\mathrm{K}}(j\omega) = \bar{\mathbf{\Delta}}_{\mathrm{K}}(j\omega).$$

Therefore, the condition that $\mathbf{\Delta}_{\mathrm{E}}(j\omega)$ excludes the origin can be replaced by the sufficient condition that $\bar{\mathbf{\Delta}}_{\mathrm{K}}(j\omega)$ exclude the origin. Since this latter set is a polytope, this condition can be verified by checking that the angle subtended by the set $\mathbf{\Delta}_{\mathrm{K}}(j\omega)$ at the origin, $\Phi_{\mathbf{\Delta}_{\mathrm{K}}}(j\omega)$ is less than π radians. Therefore we have proved the following result.

Theorem 11.4 *The family $\mathbf{\Delta}(s)$ is Hurwitz stable if it contains at least one stable polynomial and satisfies*

1) $0 \notin co\ \mathbf{\Delta}(j\omega)$ *for some* ω

2) $\Phi_{\mathbf{\Delta}_{\mathrm{K}}}(j\omega) < \pi, \qquad$ for all $\omega \in [0,\infty)$.

This result states that the Hurwitz stability of $\mathbf{\Delta}(s)$ can be determined by checking the phase difference of the vertex polynomials corresponding to the Kharitonov polynomials along the $j\omega$ axis. This is useful in view of the fact that the number of Kharitonov vertices is fixed whereas the vertices of $\mathbf{\Pi}$ increase exponentially with the dimension of the parameter space. We illustrate these results with examples.

Example 11.2. Consider the interconnected feedback system shown in Figure 11.2.

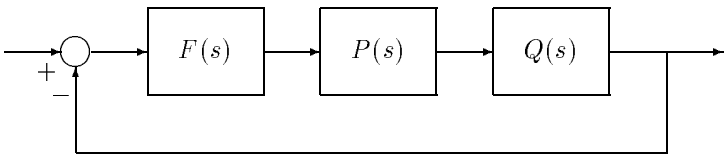

Figure 11.2. Interconnected Feedback System (Example 11.2)

Let

$$F(s) := \frac{F_1(s)}{F_2(s)} = \frac{s+2}{s+1},$$
$$P(s) := \frac{P_1(s)}{P_2(s)} = \frac{s^2+s+1}{s^3+a_2s^2+4s+a_0},$$
$$Q(s) := \frac{Q_1(s)}{Q_2(s)} = \frac{6.6s^3+13.5s^2+15.5s+20.4}{s^3+b_2s^2+3.5s+2.4}$$

and let the set of parameters $\mathbf{p} = [a_2, a_0, b_2]$ vary as follows:

$$a_2 \in [a_2^-, a_2^+] = [-3.625, -2.375],$$
$$a_0 \in [a_0^-, a_0^+] = [1.375, 2.625]$$
$$b_2 \in [b_2^-, b_2^+] = [2.875, 4.125].$$

The characteristic polynomial of the system is:

$$\begin{aligned}\delta(s,\mathbf{p}) = s^7 &+ (7.6+a_2+b_2)s^6\\ &+(40.8+a_2+b_2+a_2b_2)s^5\\ &+(85.7+a_0+3.5a_2+4b_2+a_2b_2)s^4\\ &+(137+a_0+5.9a_2+4b_2+a_0b_2)s^3\\ &+(158.3+3.5a_0+2.4a_2+a_0b_2)s^2\\ &+(101.8+5.9a_0)s+(40.8+2.4a_0).\end{aligned}$$

We verify that the following polynomial in the family is Hurwitz:

$$\begin{aligned}\delta(s,\mathbf{p}=[-3,2,3.5]) = s^7 &+ 8.1s^6+30.8s^5+80.7s^4+142.3s^3\\ &+165.1s^2+113.6s+45.6\end{aligned}$$

The parameter sets corresponding to the Kharitonov polynomials are

$$\left\{(a_2^+, a_0^-, b_2^+), (a_2^-, a_0^+, b_2^+), (a_2^+, a_0^-, b_2^-), (a_2^-, a_0^+, b_2^-)\right\}.$$

The set of Kharitonov vertex polynomials is

$$\mathbf{\Delta}_{\mathrm{K}}(s) = \{\delta_{K_1}(s), \delta_{K_2}(s), \delta_{K_3}(s), \delta_{K_4}(s)\}$$

where

$$\begin{aligned}\delta_{K_1}(s) &= s^7+9.35s^6+32.7531s^5+85.4656s^4+146.5344s^3+163.0844s^2\\ &\quad +109.9125s+44.1\\ \delta_{K_2}(s) &= s^7+8.10s^6+34.4719s^5+83.4344s^4+139.8156s^3+161.3656s^2\\ &\quad +109.9125s+44.1\\ \delta_{K_3}(s) &= s^7+8.10s^6+26.3469s^5+77.1844s^4+145.5656s^3+169.6156s^2\\ &\quad +117.2875s+47.1\\ \delta_{K_4}(s) &= s^7+6.85s^6+29.6281s^5+76.7156s^4+137.2844s^3+166.3344s^2\\ &\quad +117.2875s+47.1\end{aligned}$$

One approach is to check the Hurwitz stability of all convex combinations of these polynomials. This in turn can be done by using the Segment Lemma (Chapter 2). Alternatively, we may check the phase differences of these vertex polynomials. If the maximum phase difference is less than 180° (π radians) for all ω, the origin is excluded from convex hull of $\mathbf{\Delta}_{\mathrm{E}}(j\omega)$ for all ω. We show the convex hulls of image sets in Figure 11.3 for illustration.

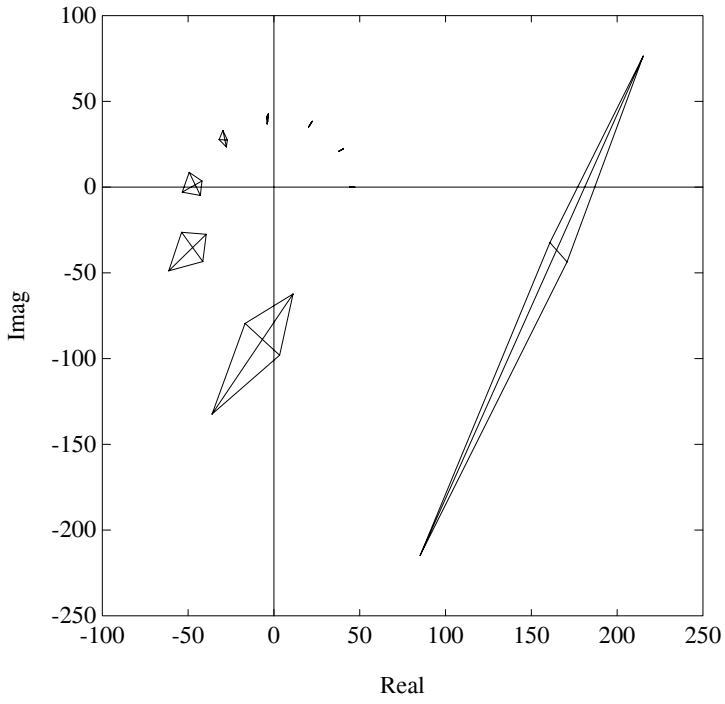

Figure 11.3. Convex hulls of image sets (Example 11.2)

We confirm robust stability by verifying (see Figure 11.4) the maximum phase difference never reaches 180° for all ω. We also note that if we had applied the Mapping Theorem directly to the three dimensional parameter space $\mathbf{p}$, we would have had to check 8 vertices as opposed to the 4 vertices checked here. This reduction is due to the application of the multilinear version of the Generalized Kharitonov Theorem.

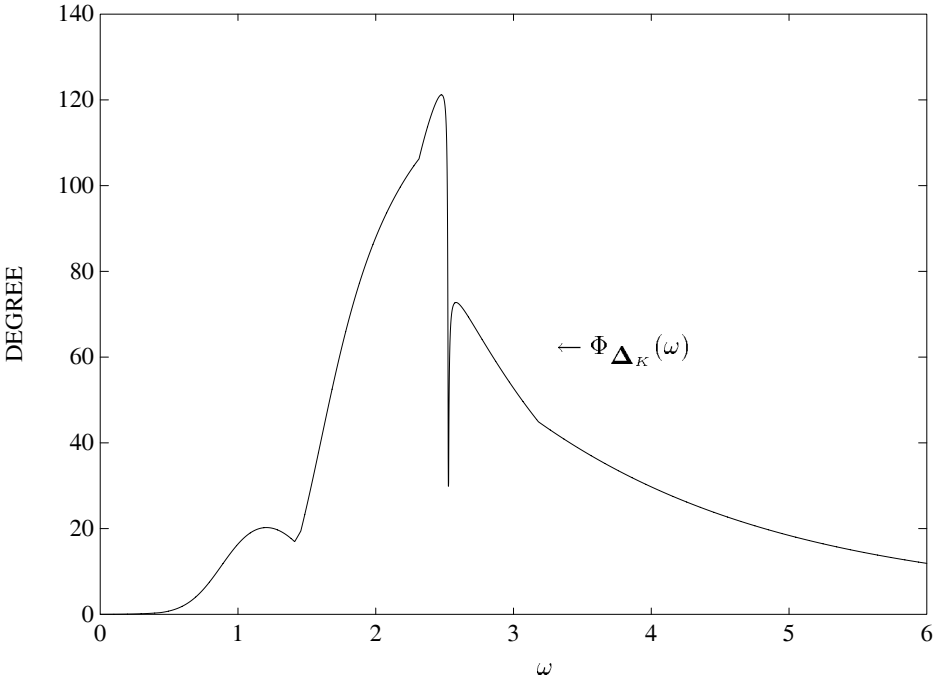

Figure 11.4. $\Phi_{\mathbf{\Delta}_K}(\omega)$ vs. ω (Example 11.2)

11.3 PARAMETRIC STABILITY MARGIN

Consider again the family of polynomials

$$\mathbf{\Delta}(s) = F_1(s)\mathbf{P}_{11}(s)\cdots\mathbf{P}_{1r_1}(s) + \cdots + F_m(s)\mathbf{P}_{m1}(s)\cdots\mathbf{P}_{mr_m}(s). \tag{11.22}$$

Let $\mathbf{p}_{ij}$ denote the vector of coefficients of the polynomials $P_{ij}(s)$. Each such coefficient belongs to a given interval and the corresponding box of parameters is denoted by $\mathbf{\Pi}_{ij}$. Then the box of uncertain parameters is

$$\mathbf{\Pi} := \mathbf{\Pi}_{11} \times \mathbf{\Pi}_{12} \times \cdots \times \mathbf{\Pi}_{mr_m}. \tag{11.23}$$

The extremal manifolds $\mathbf{\Delta}_{\mathrm{E}}(s)$ are defined as follows:

$$\begin{aligned}\mathbf{\Delta}^l_{\mathrm{E}}(s) := {} & F_1(s)\mathcal{K}_{11}(s)\cdots\mathcal{K}_{1r_1}(s) + \cdots + F_{l-1}(s)\mathcal{K}_{l-1,1}(s)\cdots\mathcal{K}_{l-1,r_{l-1}}(s) \\ & + F_l(s)\mathcal{S}_{l,1}(s)\cdots\mathcal{S}_{l,r_l}(s) + F_{l+1}\mathcal{K}_{l+1,1}(s)\cdots\mathcal{K}_{l+1,r_{l+1}} \\ & + \cdots + F_m(s)\mathcal{K}_{m,1}(s)\cdots\mathcal{K}_{m,r_m}(s)\end{aligned} \tag{11.24}$$

$$\mathbf{\Delta}_{\mathrm{E}}(s) := \cup_{l=1}^{m}\mathbf{\Delta}^l_{\mathrm{E}}(s). \tag{11.25}$$

The parameter space subsets corresponding to $\mathbf{\Delta}_{\mathrm{E}}^{l}(s)$ and $\mathbf{\Delta}_{\mathrm{E}}(s)$ are denoted by $\mathbf{\Pi}_l$ and

$$\mathbf{\Pi}_{\mathrm{E}} := \bigcup_{l=1}^{m} \mathbf{\Pi}_l. \tag{11.26}$$

Let $\mathbf{\Pi}_{\mathrm{K}}$ denote the parameter vector set corresponding to the case where each polynomial $P_{ij}(s)$ set to a corresponding Kharitonov polynomial. We write

$$\begin{aligned}
\mathbf{\Delta}(s) &= \{\delta(s,\mathbf{p}) \ : \ \mathbf{p} \in \mathbf{\Pi}\} \\
\mathbf{\Delta}_{\mathrm{E}}(s) &= \{\delta(s,\mathbf{p}) \ : \ \mathbf{p} \in \mathbf{\Pi}_{\mathrm{E}}\} \\
\mathbf{\Delta}_{\mathrm{K}}(s) &= \{\delta(s,\mathbf{p}) \ : \ \mathbf{p} \in \mathbf{\Pi}_{\mathrm{K}}\}.
\end{aligned}$$

In this section, we show that for the family $\mathbf{\Delta}(s)$ in (11.22) the worst case parametric stability margin over the uncertainty box $\mathbf{\Pi}$ occurs, in fact, on the set $\mathbf{\Pi}_{\mathrm{E}}$.

Let $\|\cdots\|$ denote any norm in $\mathbb{R}^n$ and let $\mathcal{P}_u$ denote the set of points $\mathbf{u}$ in $\mathbb{R}^n$ for which $\delta(s,\mathbf{u})$ is unstable or loses degree (relative to its degree over $\mathbf{\Pi}$). Let

$$\rho(\mathbf{p}) = \inf_{\mathbf{u}\in\mathcal{P}_u} \|\mathbf{p}-\mathbf{u}\|_p$$

denote the radius of the stability ball (measured in the norm $\|\cdot\|$) and centered at the point $\mathbf{p}$. This number serves as the stability margin associated with the point $\mathbf{p}$. If the box $\mathbf{\Pi}$ is stable we can associate a stability margin with each point in $\mathbf{\Pi}$. A natural question to ask is: What is the worst case stability margin in the norm $\|\cdot\|$ as $\mathbf{p}$ ranges over $\mathbf{\Pi}$? The answer to that question is provided in the following theorem.

Theorem 11.5 (Extremal Parametric Stability Margin)

$$\inf_{\mathbf{p}\in\mathbf{\Pi}} \rho(\mathbf{p}) = \inf_{\mathbf{p}\in\mathbf{\Pi}_{\mathrm{E}}} \rho(\mathbf{p}). \tag{11.27}$$

Proof. Since $\mathbf{\Delta}(j\omega)$ and $\mathbf{\Delta}_E(j\omega)$ have the same boundary,

$$\begin{aligned}
\inf_{\mathbf{p}\in\mathbf{\Pi}} \rho(\mathbf{p}) &= \inf_{\mathbf{p}\in\mathbf{\Pi}} \inf_{\mathbf{u}\in\mathcal{P}_u} \|\mathbf{p}-\mathbf{u}\|_p \\
&= \inf\{\|\mathbf{a}\| : \delta(j\omega,\mathbf{p}+\mathbf{a}) = 0, \quad \mathbf{p}\in\mathbf{\Pi}, \quad \omega\in[-\infty,+\infty]\} \\
&= \inf\{\|\mathbf{a}\| : \delta(j\omega,\mathbf{p}+\mathbf{a}) = 0, \quad \mathbf{p}\in\mathbf{\Pi}_{\mathrm{E}}, \quad \omega\in[-\infty,+\infty]\} \\
&= \inf_{\mathbf{p}\in\mathbf{\Pi}_{\mathrm{E}}} \inf_{\mathbf{u}\in\mathcal{P}_u} \|\mathbf{p}-\mathbf{u}\|_p = \inf_{\mathbf{p}\in\mathbf{\Pi}_{\mathrm{E}}} \rho(\mathbf{p}).
\end{aligned} \tag{11.28}$$

♣

Example 11.3. Consider the system in Example 11.2 with nominal values

$$a_2^0 = -3, \quad a_0^0 = 2, \quad b_2^0 = 3.5.$$

We compute the maximum parametric stability margin ϵ^* around the nominal values as follows:

$$a_2 \in [a_2^0 - \epsilon, a_2^0 + \epsilon], \quad a_0 \in [a_0^0 - \epsilon, a_0^0 + \epsilon], \quad b_2 \in [b_2^0 - \epsilon, b_2^0 + \epsilon].$$

From the four vertices given in Example 11.2, we have six segments bounding the convex hull of the images. To check the stability of these segments, we apply the Segment Lemma (Chapter 2) with incremental steps of ϵ. This gives $\epsilon^* = 0.63$. The image set of the characteristic polynomial with ϵ^* is shown in Figure 11.5. The figure shows that the image set is almost touching the origin and thus $\epsilon^* = 0.63$ is the parametric stability margin.

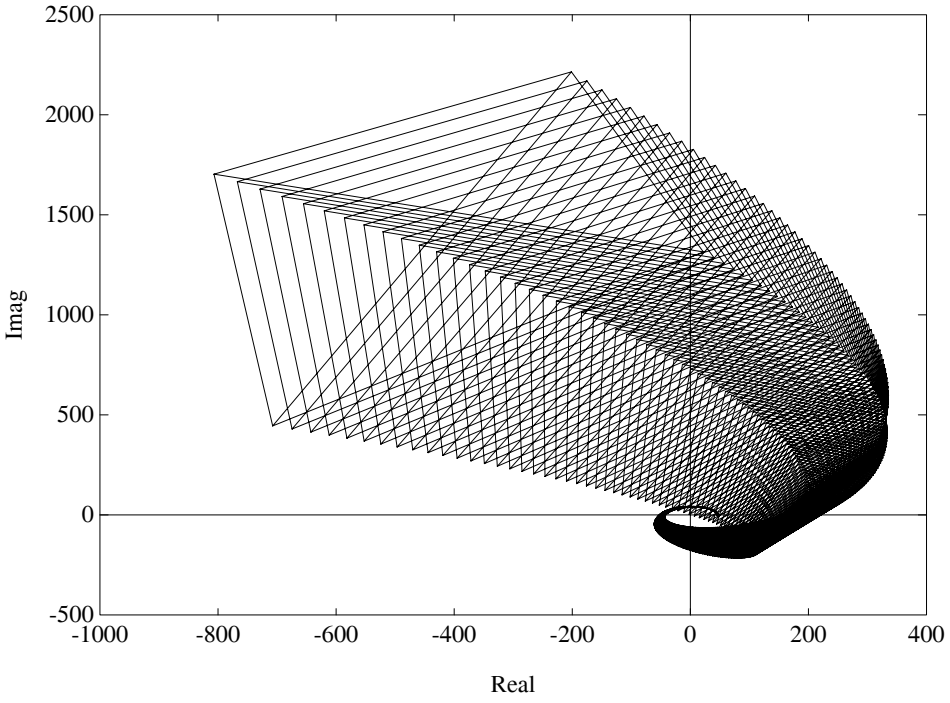

Figure 11.5. Image set for $\epsilon = 0.63$ (Example 11.3)

11.4 MULTILINEAR INTERVAL SYSTEMS

In the rest of this chapter, we will be dealing with transfer functions containing interval parameters with multilinear dependency. The transfer function in question could be embedded in a feedback control system and we will be interested in determining robust stability as well as worst case stability margins and performance

measures of such systems. We begin by first focussing on a *multilinear interval system*, namely one whose transfer function is a ratio of multilinear polynomials with independent parameters. To be specific we will consider single-input, single-output, proper, stable systems with transfer function of the form

$$G(s) = \frac{\gamma(s)}{\delta(s)}.$$

Here

$$\gamma(s) = H_1(s)L_{11}(s)L_{12}(s)\cdots L_{1r_1}(s) + \cdots\cdots + H_m(s)L_{m1}(s)L_{m2}(s)\cdots L_{mr_m}(s)$$

where the polynomials $H_i(s)$ are fixed and the polynomials $L_{ij}(s) \in \mathbf{L}_{ij}(s)$ are independent real interval polynomials. Let $\mathbf{l}$ denote the ordered set of coefficients of the interval polynomials; $\mathbf{l}$ varies in a prescribed axis parallel box $\mathbf{\Lambda}$; the corresponding family of polynomials $\gamma(s)$ is denoted by $\mathbf{\Gamma}(s)$. Similarly we suppose that

$$\delta(s) = F_1(s)P_{11}(s)P_{12}(s)\cdots P_{1r_1}(s) + \cdots\cdots + F_m(s)P_{m1}(s)P_{m2}(s)\cdots P_{mr_m}(s)$$

where the polynomials $F_i(s)$ are fixed, the polynomials $P_{ij}(s)$ are real interval polynomials with the vector of coefficients denoted by $\mathbf{p}$ varying in the prescribed box $\mathbf{\Pi}$. The resulting family of polynomials $\delta(s)$ is denoted $\mathbf{\Delta}(s)$. We also denote explicitly the dependence of $\delta(s)$ on $\mathbf{p}$ and of $\nu(s)$ on $\mathbf{l}$ by writing $\delta(s,\mathbf{p})$ and $\nu(s,\mathbf{l})$ whenever necessary. We make the standing assumption.

Assumption 11.1.

A1) Parameters $\mathbf{p}$ and $\mathbf{l}$ are independent.

A2) $\gamma(s,\mathbf{l})$ and $\delta(s,\mathbf{p})$ are coprime over $(\mathbf{p},\mathbf{l}) \in \mathbf{\Pi} \times \mathbf{\Lambda}$.

A3) $\delta(j\omega,\mathbf{p}) \neq 0$ for all $\mathbf{p} \in \mathbf{\Pi}$ and each $\omega > 0$.

Later in this section we show how to deal with the situations when assumption A1 does not hold. To display the dependence of a typical element $G(s)$ of $\mathbf{G}$ on $\mathbf{l}$ and $\mathbf{p}$ we write it as $G(s,\mathbf{p},\mathbf{l})$:

$$G(s,\mathbf{p},\mathbf{l}) = \frac{\gamma(s,\mathbf{l})}{\delta(s,\mathbf{p})} \tag{11.29}$$

We form the parametrized family of transfer functions

$$\mathbf{G}(s) = \{G(s,\mathbf{p},\mathbf{l}) \ : \ (\mathbf{p},\mathbf{l}) \in (\mathbf{\Pi} \times \mathbf{\Lambda})\} = \frac{\mathbf{\Gamma}(s)}{\mathbf{\Delta}(s)}. \tag{11.30}$$

In order to apply frequency domain methods of analysis and design to the family of systems $\mathbf{G}(s)$ it is necessary to obtain the image set $\mathbf{G}(j\omega)$. We first show how the boundary of this set can be evaluated. We proceed as in the linear case by determining an extremal multilinear interval family of systems $\mathbf{G}_{\mathrm{E}}(s)$. Introduce

the Kharitonov polynomials and segments associated with the $P_{ij}(s)$ and $L_{ij}(s)$ respectively, and construct the extremal polynomial manifolds $\mathbf{\Delta}_{\rm E}(s)$ and $\mathbf{\Gamma}_{\rm E}(s)$ and the vertex sets $\mathbf{\Delta}_{\rm K}(s)$ and $\mathbf{\Gamma}_{\rm K}(s)$ as in Section 11.2. Let $\mathbf{\Pi}_{\rm E}$, $\mathbf{\Lambda}_{\rm E}$ and $\mathbf{\Pi}_{\rm K}$, $\mathbf{\Lambda}_{\rm K}$ denote the corresponding manifolds and vertices in $\mathbf{\Pi}$ and $\mathbf{\Lambda}$ respectively:

$$\mathbf{\Gamma}_{\rm E}(s) = \{\gamma(s,\mathbf{l}) : \mathbf{l} \in \mathbf{\Lambda}_{\rm E}\}, \qquad \mathbf{\Gamma}_{\rm K}(s) = \{\gamma(s,\mathbf{l}) : \mathbf{l} \in \mathbf{\Lambda}_{\rm K}\}$$

$$\mathbf{\Delta}_{\rm E}(s) = \{\delta(s,\mathbf{p}) : \mathbf{p} \in \mathbf{\Pi}_{\rm E}\}, \qquad \mathbf{\Delta}_{\rm K}(s) = \{\delta(s,\mathbf{p}) : \mathbf{p} \in \mathbf{\Pi}_{\rm K}\}.$$

The *extremal set* $\mathbf{G}_{\rm E}(s)$ is then defined as

$$\mathbf{G}_{\rm E}(s) := \left\{ \frac{\gamma(s,\mathbf{l})}{\delta(s,\mathbf{p})} : (\mathbf{l} \in \mathbf{\Lambda}_{\rm K},\ \mathbf{p} \in \mathbf{\Pi}_{\rm E}) \text{ or } (\mathbf{l} \in \mathbf{\Lambda}_{\rm E},\ \mathbf{p} \in \mathbf{\Pi}_{\rm K}) \right\}. \tag{11.31}$$

Using our compact notational convention we can write

$$\mathbf{G}_{\rm E}(s) = \left(\frac{\mathbf{\Gamma}_{\rm K}(s)}{\mathbf{\Delta}_{\rm E}(s)}\right) \cup \left(\frac{\mathbf{\Gamma}_{\rm E}(s)}{\mathbf{\Delta}_{\rm K}(s)}\right).$$

Theorem 11.6 *Under the Assumption 11.1,*

$$\partial\mathbf{G}(j\omega) \subset \mathbf{G}_{\rm E}(j\omega)$$

for all $\omega \in [0,\infty)$.

Proof. The Assumption A3 guarantees that the set $\mathbf{G}(j\omega)$ is well defined. The proof of the theorem now follows from the boundary properties of the sets $\mathbf{\Delta}_{\rm E}(j\omega)$ and $\mathbf{\Gamma}_{\rm E}(j\omega)$, and the independence of the parameter $\mathbf{p}$ and $\mathbf{l}$. We know that

$$\begin{aligned} z \in \partial\mathbf{G}(j\omega) &= \partial\left(\frac{\mathbf{\Gamma}(j\omega)}{\mathbf{\Delta}(j\omega)}\right) \\ &\Leftrightarrow 0 \in \partial\left(\mathbf{\Gamma}(j\omega) - z\mathbf{\Delta}(j\omega)\right) \\ &\Leftrightarrow 0 \in \left(\mathbf{\Gamma}_{\rm K}(j\omega) - z\mathbf{\Delta}_{\rm E}(j\omega)\right) \cup \left(\mathbf{\Gamma}_{\rm E}(j\omega) - z\mathbf{\Delta}_{\rm K}(j\omega)\right) \\ &\Leftrightarrow z \in \left(\frac{\mathbf{\Gamma}_{\rm K}(j\omega)}{\mathbf{\Delta}_{\rm E}(j\omega)}\right) \cup \left(\frac{\mathbf{\Gamma}_{\rm E}(j\omega)}{\mathbf{\Delta}_{\rm K}(j\omega)}\right) = \mathbf{G}_{\rm E}(j\omega). \end{aligned}$$

♣

The proof given above and the formula for the boundary parallels the linear case treated in Chapter 8.

Now suppose that $G(s)$ is part of the control system shown in Figure 11.6.

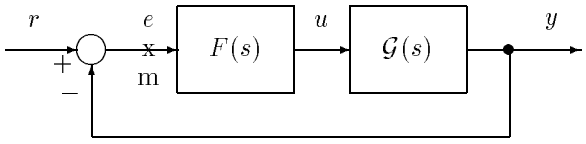

Figure 11.6. A unity feedback system

Define transfer functions:

$$\frac{y(s)}{u(s)} = G(s), \qquad \frac{u(s)}{e(s)} = F(s), \tag{11.32}$$

$$T^o(s) := \frac{y(s)}{e(s)} = F(s)G(s), \qquad T^e(s) := \frac{e(s)}{r(s)} = \frac{1}{1+F(s)G(s)}, \tag{11.33}$$

$$T^u(s) := \frac{u(s)}{r(s)} = \frac{F(s)}{1+F(s)G(s)}, \qquad T^y(s) := \frac{y(s)}{r(s)} = \frac{F(s)G(s)}{1+F(s)G(s)}. \tag{11.34}$$

As $G(s)$ ranges over the uncertainty set $\mathbf{G}(s)$, these transfer functions vary in corresponding sets.

$$\begin{aligned}
\mathbf{T}^o(s) &:= \{F(s)G(s) \ : \ G(s) \in \mathbf{G}(s)\} \\
\mathbf{T}^e(s) &:= \left\{ \frac{1}{1+F(s)G(s)} \ : \ G(s) \in \mathbf{G}(s) \right\} \\
\mathbf{T}^u(s) &:= \left\{ \frac{F(s)}{1+F(s)G(s)} \ : \ G(s) \in \mathbf{G}(s) \right\} \\
\mathbf{T}^y(s) &:= \left\{ \frac{F(s)G(s)}{1+F(s)G(s)} \ : \ G(s) \in \mathbf{G}(s) \right\}.
\end{aligned} \tag{11.35}$$

It turns out that the boundary of the image set, at $s = j\omega$, of each of the above sets is generated by the extremal set $\mathbf{G}_{\mathrm{E}}(s)$. Introduce the *extremal subsets*:

$$\mathbf{T}^o_{\mathrm{E}}(s) := \{F(s)G(s) \ : \ G(s) \in \mathbf{G}_{\mathrm{E}}(s)\} \tag{11.36}$$

$$\mathbf{T}^e_{\mathrm{E}}(s) := \left\{ \frac{1}{1+F(s)G(s)} \ : \ G(s) \in \mathbf{G}_{\mathrm{E}}(s) \right\} \tag{11.37}$$

$$\mathbf{T}^u_{\mathrm{E}}(s) := \left\{ \frac{F(s)}{1+F(s)G(s)} \ : \ G(s) \in \mathbf{G}_{\mathrm{E}}(s) \right\} \tag{11.38}$$

$$\mathbf{T}^y_{\mathrm{E}}(s) := \left\{ \frac{F(s)G(s)}{1+F(s)G(s)} \ : \ G(s) \in \mathbf{G}_{\mathrm{E}}(s) \right\}. \tag{11.39}$$

Theorem 11.7 *For every* $\omega \geq 0$,

$$\begin{array}{ll} (a) & \partial \mathbf{T}^o(j\omega) \subset \mathbf{T}^o_{\mathrm{E}}(j\omega) \\ (b) & \partial \mathbf{T}^e(j\omega) \subset \mathbf{T}^e_{\mathrm{E}}(j\omega) \\ (c) & \partial \mathbf{T}^u(j\omega) \subset \mathbf{T}^u_{\mathrm{E}}(j\omega) \\ (d) & \partial \mathbf{T}^y(j\omega) \subset \mathbf{T}^y_{\mathrm{E}}(j\omega) \end{array}$$

The proof of the above relations can be carried out in a manner identical to the proof of Theorem 8.3 in the linear case (Chapter 8) and is therefore omitted. In fact, all the boundary results related to the Nyquist and Bode envelopes proved in Chapter 8 carry over to the multilinear case with the corresponding extremal set $\mathbf{G}_{\mathrm{E}}(s)$. In the following subsection we show that these boundary results hold for a much larger class of functions of $\mathbf{G}(s)$.

11.4.1 Extensions of Boundary Results

In defining our multilinear interval system we had assumed that the numerator and denominator parameters of $G(s)$ are independent. However for closed loop transfer functions this assumption of independence does not hold. Nevertheless the boundary generating property of the set $\mathbf{G}_{\mathrm{E}}(s)$ still holds for these closed loop transfer functions. It is natural to attempt to generalize this boundary generating property to a large class of functions where dependencies between numerator and denominator parameters occur. Such dependencies invariably occur in the transfer functions associated with multiloop control systems. We begin with a multilinear function $Q(s)$ of several transfer functions $G^i(s), i = 1, 2 \cdots, q$. Let us assume that each $G^i(s)$ itself lies in a multilinear interval family of systems $\mathbf{G}^i(s)$ defined as in this section, with independent parameters in the numerator and denominator. We also assume that the parameters in $G^i(s)$ are independent of those in $G^j(s)$, $i \neq j$. Note that if we regard $Q(s)$ as a rational function its numerator and denominator polynomials contain common interval parameters. Let

$$\mathbf{Q}(s) := \{Q(s) : G^i(s) \in \mathbf{G}^i(s), \quad i = 1, 2 \cdots q\}.$$

We wish to determine the complex plane image set of the family $\mathbf{Q}(s)$ evaluated at $s = j\omega$:

$$\mathbf{Q}(j\omega) := \{Q(j\omega) : G^i(s) \in \mathbf{G}^i(s), \quad i = 1, 2 \cdots q\}.$$

Let $\mathbf{G}^i_{\mathrm{E}}(s)$ denote the extremal subset of $\mathbf{G}^i(s)$ and introduce

$$\mathbf{Q}_{\mathrm{E}}(j\omega) := \{Q(j\omega) : G^i(s) \in \mathbf{G}^i_{\mathrm{E}}(s), \quad i = 1, 2 \cdots q\}.$$

Then we can state the following boundary result.

Theorem 11.8

$$\partial \mathbf{Q}(j\omega) \subset \mathbf{Q}_{\mathrm{E}}(j\omega). \tag{11.40}$$

Proof. Let us introduce the complex numbers $s_i = G^i(j\omega)$ and the corresponding sets

$$\mathcal{Z}_i := \{G^i(j\omega) : G^i(s) \in \mathbf{G}^i(s), \quad i = 1, 2 \cdots q\}.$$

Since sums and products of complex plane sets satisfy the following boundary properties

$$\begin{aligned} \partial(\mathcal{Z}_i + \mathcal{Z}_j) &\subseteq \partial\mathcal{Z}_i + \partial\mathcal{Z}_j, \qquad (i \neq j) \\ \partial(\mathcal{Z}_i \cdot \mathcal{Z}_j) &\subseteq \partial\mathcal{Z}_i \cdot \partial\mathcal{Z}_j, \qquad (i \neq j). \end{aligned}$$

and

$$\partial\mathcal{Z}_i \subset \mathbf{G}^i_{\mathrm{E}}(j\omega), \qquad i = 1, 2 \cdots, q.$$

the multilinearity of the function $Q(s)$ gives us the conclusion stated. ♣

We can generalize the above property even further. Let $Q(s)$ be as above and consider a linear fractional transformation (LFT) $T(Q(s))$ defined by arbitrary functions $A(s), B(s), C(s)$ and $D(s)$

$$T(Q(s)) := Q_1(s) := \frac{A(s)Q(s) + B(s)}{C(s)Q(s) + D(s)}.$$

Introduce the set

$$T(\mathbf{Q}(s)) := \left\{ \frac{A(s)Q(s) + B(s)}{C(s)Q(s) + D(s)} : Q(s) \in \mathbf{Q}(s) \right\}.$$

Let us now impose the restriction

$$A(j\omega)D(j\omega) - B(j\omega)C(j\omega) \neq 0. \tag{11.41}$$

Under the above restriction $T(Q(j\omega))$ is a LFT of $Q(j\omega)$ and thus carries boundaries onto boundaries. Thus we know that the boundary of $\mathbf{Q}_1(j\omega)$ is also generated by the extremal systems $\mathbf{G}^i_{\mathrm{E}}(s)$.

Theorem 11.9 *Let $\mathbf{Q}(s)$ be as defined above and let $T(Q(s))$ be an LFT. Then, assuming (11.41) holds*

$$\partial T(\mathbf{Q}(j\omega)) \subset T(\mathbf{Q}_{\mathrm{E}}(j\omega)).$$

Remark 11.2. We remark that any LFT of $Q_1(s)$ as well as sums and products of LFT's continue to enjoy the boundary generating property of the extremal systems. In this way a large class of transfer functions occurring in closed loop systems can be handled.

Computation of $\mathbf{G}_{\mathrm{E}}(j\omega)$

As we have seen, the determination of the set $\mathbf{G}(j\omega)$ reduces to evaluating $\mathbf{G}_{\mathrm{E}}(j\omega)$, a set of smaller dimension. Nevertheless, $\mathbf{G}_{\mathrm{E}}(j\omega)$ is still a multilinear function of the uncertain segment parameters. The only way to exactly evaluate this set is by gridding over the uncertainty box. In general this procedure is computationally expensive or even infeasible. Fortunately, as we have seen earlier, the "concave" property of the image set of multilinear interval polynomials given by the Mapping Theorem allows us to overbound $\mathbf{G}_{\mathrm{E}}(j\omega)$ by a ratio of unions of convex polygons. Recall that

$$\mathbf{G}_{\mathrm{E}}(j\omega) = \left(\frac{\mathbf{\Gamma}_{\mathrm{K}}(j\omega)}{\mathbf{\Delta}_{\mathrm{E}}(j\omega)}\right) \cup \left(\frac{\mathbf{\Gamma}_{\mathrm{E}}(j\omega)}{\mathbf{\Delta}_{\mathrm{K}}(j\omega)}\right). \tag{11.42}$$

From the Mapping Theorem we have

$$\mathbf{\Gamma}_{\mathrm{E}}(j\omega) \subset co\ \mathbf{\Gamma}_{\mathrm{K}}(j\omega)$$
$$\mathbf{\Delta}_{\mathrm{E}}(j\omega) \subset co\ \mathbf{\Delta}_{\mathrm{K}}(j\omega).$$

Now consider $\bar{\mathbf{G}}_{\mathrm{E}}(j\omega)$ defined by replacing $\mathbf{\Gamma}_{\mathrm{E}}(j\omega)$ and $\mathbf{\Delta}_{\mathrm{E}}(j\omega)$ by $co\ \mathbf{\Gamma}_{\mathrm{K}}(j\omega)$ and $co\ \mathbf{\Delta}_{\mathrm{K}}(j\omega)$ respectively. In other words,

$$\bar{\mathbf{G}}_{\mathrm{E}}(j\omega) = \left(\frac{\mathbf{\Gamma}_{\mathrm{K}}(j\omega)}{co\ \mathbf{\Delta}_{\mathrm{K}}(j\omega)}\right) \cup \left(\frac{co\ \mathbf{\Gamma}_{\mathrm{K}}(j\omega)}{\mathbf{\Delta}_{\mathrm{K}}(j\omega)}\right). \tag{11.43}$$

It is clear that $\bar{\mathbf{G}}_{\mathrm{E}}(j\omega)$ overbounds $\mathbf{G}_{\mathrm{E}}(j\omega)$:

$$\mathbf{G}_{\mathrm{E}}(j\omega) \subset \bar{\mathbf{G}}_{\mathrm{E}}(j\omega). \tag{11.44}$$

The evaluation of $\bar{\mathbf{G}}_{\mathrm{E}}(j\omega)$ is relatively easy because it consists of a union of one-parameter families of transfer functions of the types

$$\frac{\lambda U_1(j\omega) + (1-\lambda)U_2(j\omega)}{V(j\omega)} \quad \text{or} \quad \frac{U(j\omega)}{\lambda V_1(j\omega) + (1-\lambda)V_2(j\omega)}.$$

The union of these one-parameter families gives rise to $\bar{\mathbf{G}}_{\mathrm{E}}(j\omega)$ which overbounds the boundary of $\mathbf{G}(j\omega)$. The tightness of the approximation can be improved as we have seen before, by introducing additional vertices in the parameter set $\mathbf{\Pi} \times \mathbf{\Lambda}$. The guaranteed gain and phase margins of a control system containing parameter uncertainty may be obtained from these overbounded sets as shown in Figure 11.7. The image at $s = j\omega$ of each of the transfer function sets associated with the feedback system considered in Figure 11.6 can be overbounded by replacing $\mathbf{G}(j\omega)$ by $\bar{\mathbf{G}}_{\mathrm{E}}(j\omega)$, and in fact we can do the same for any linear fractional transformation of $G(s)$. An example of this calculation follows.

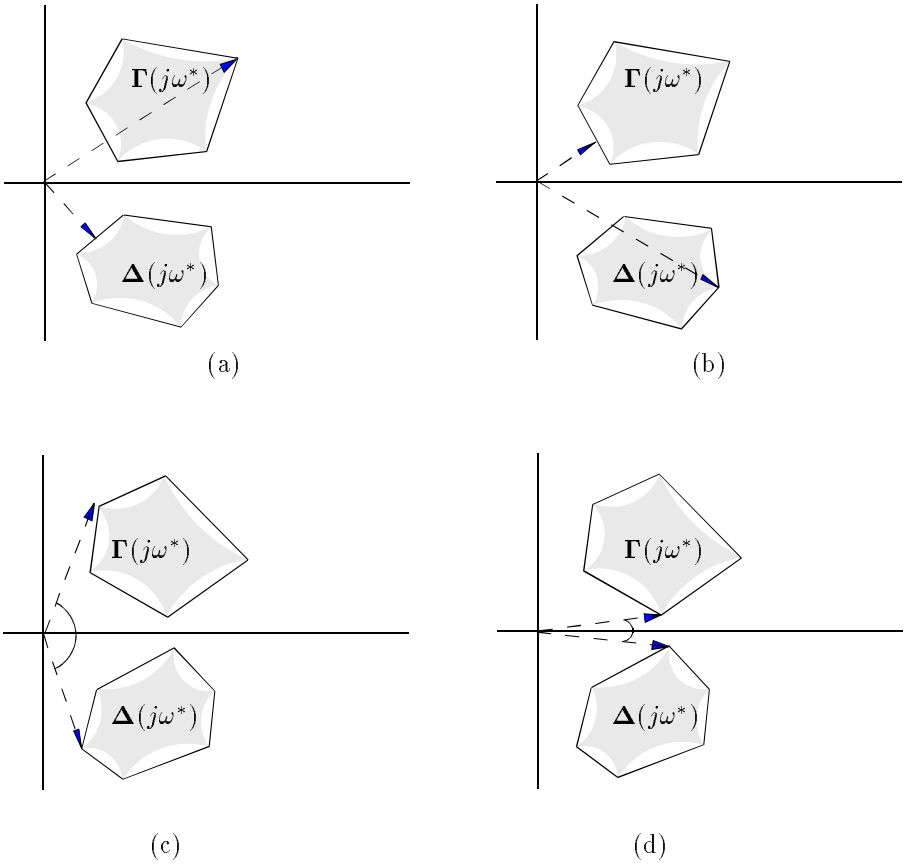

Figure 11.7. Guaranteed gain and phase margin using overbounded sets

Example 11.4. (Nyquist, Bode and Nichols Envelopes of Multilinear Systems) The purpose of this example to show how to construct the frequency domain envelopes (Nyquist, Bode and Nichols envelopes) of the multilinear interval family. Let us recall the system given in Example 11.1:

$$F(s)\underbrace{P(s)Q(s)}_{G(s)} = \frac{(s+2)(s^2+s+1)(6.6s^3+13.5s^2+15.5s+20.4)}{(s+1)(s^3+a_2s^2+4s+a_0)(s^3+b_2s^2+3.5s+2.4)}$$

where

$$a_2 \in [a_2^-, a_2^+] = [-3.625, -2.375], \qquad a_0 \in [a_0^-, a_0^+] = [1.375, 2.625]$$

$$b_2 \in [b_2^-, b_2^+] = [2.875, 4.125].$$

From Theorem 11.6, it is enough to consider $\mathbf{G}_{\mathrm{E}}(j\omega)$. Since this particular example has parameters only in the denominator, we have

$$\begin{aligned}\partial\left(F(j\omega)\mathbf{G}(j\omega)\right) &\subset F(j\omega)\mathbf{G}_{\mathrm{E}}(j\omega) \\ &= \frac{(s+2)(s^2+s+1)(6.6s^3+13.5s^2+15.5s+20.4)|_{s=j\omega}}{\boldsymbol{\Delta}_{\mathrm{E}}(j\omega)}\end{aligned}$$

where $\boldsymbol{\Delta}_{\mathrm{E}}(j\omega)$ consists of the six line segments joining the following four vertices:

$$\begin{aligned}&(s+1)(s^3+a_2^+s^2+4s+a_0^-)(s^3+b_2^+s^2+3.5s+2.4)|_{s=j\omega} \\ &(s+1)(s^3+a_2^+s^2+4s+a_0^-)(s^3+b_2^-s^2+3.5s+2.4)|_{s=j\omega} \\ &(s+1)(s^3+a_2^-s^2+4s+a_0^+)(s^3+b_2^+s^2+3.5s+2.4)|_{s=j\omega} \\ &(s+1)(s^3+a_2^-s^2+4s+a_0^+)(s^3+b_2^-s^2+3.5s+2.4)|_{s=j\omega}.\end{aligned}$$

Figures 11.8, 11.9, and 11.10 are obtained accordingly.

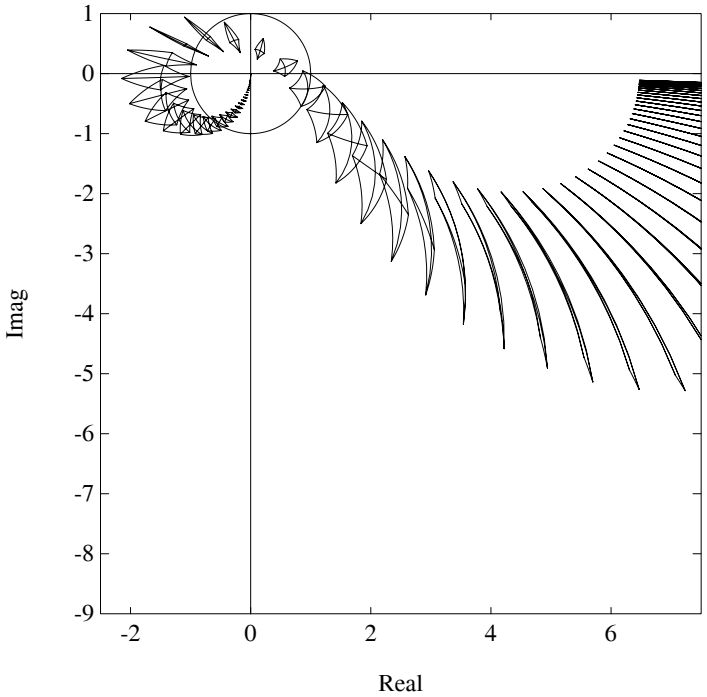

Figure 11.8. Nyquist envelope (Example 11.4)

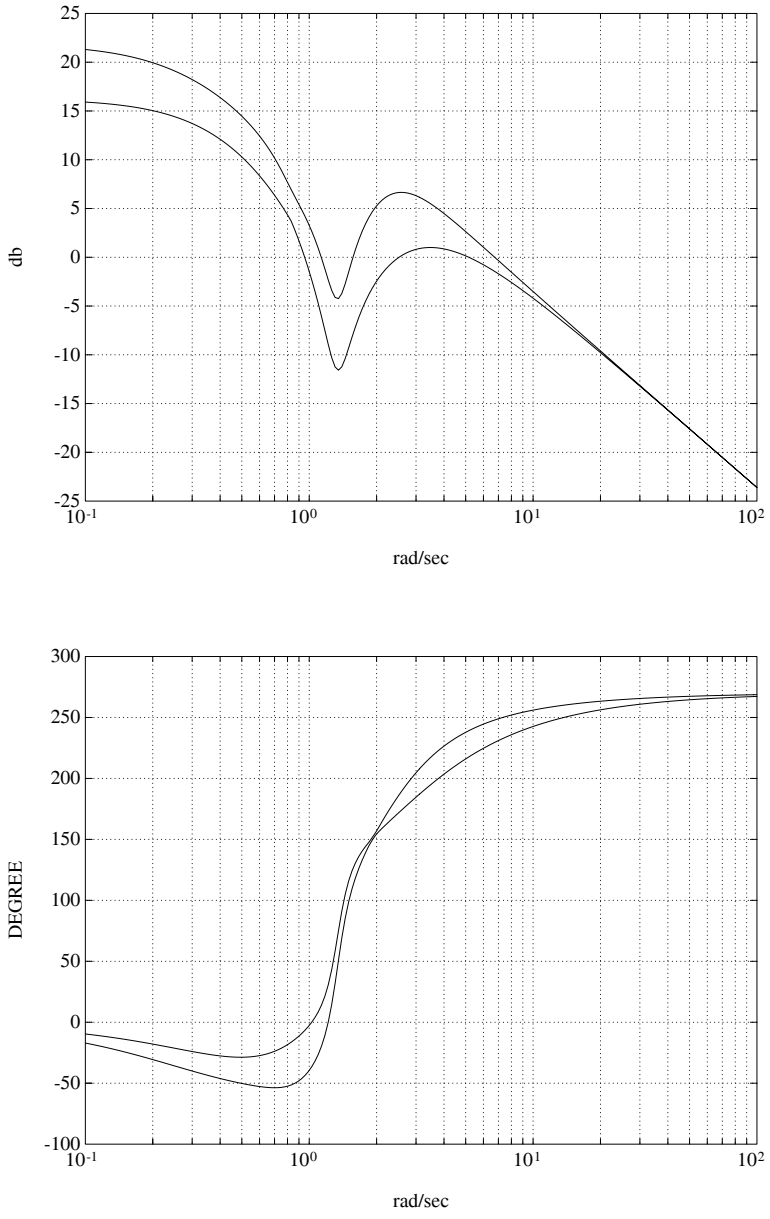

Figure 11.9. Bode magnitude and phase envelopes (Example 11.4)

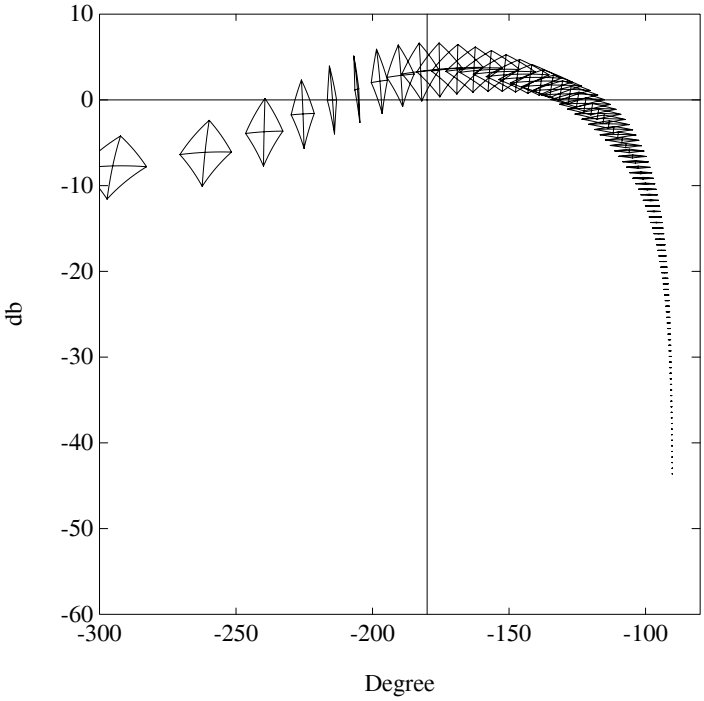

Figure 11.10. Nichols envelope (Example 11.4)

11.5 H_∞ STABILITY MARGIN

In this section we use the boundary results derived above to efficiently deal with many frequency domain measures of performance and, in particular, to determine worst case performance over the parameter set associated with a multilinear interval systems. As in Chapter 8 we will use the standard notation: $\mathbf{C}_+ := \{s \in C : \ \mathrm{Re}(s) \geq 0\}$, and $H_\infty(\mathbf{C}_+)$ will represent the space of functions $f(s)$ that are bounded and analytic in $\mathbf{C}_+$ with the standard H_∞ norm,

$$\|f\|_\infty = \sup_{\omega \in \mathbf{R}} |f(j\omega)|.$$

Let us consider the multilinear interval family of systems $\mathbf{G}(s)$ defined earlier (see (11.30)) and let us assume that the entire family is stable. To determine the unstructured stability margin of control systems containing the family $\mathbf{G}(s)$ we need to determine the supremum of the H_∞ norm of certain transfer functions over $\mathbf{G}(s)$. Since the H_∞ norm-bounded perturbations provide uniform perturbations at all frequencies, it is desirable to shape this perturbation by introducing a weight. Let

the weight $W(s)$ be a scalar stable proper transfer function

$$W(s) = \frac{n_w(s)}{d_w(s)}.$$

To start with, let us look at two specific robust stability problems involving mixed parametric-unstructured uncertainty:

Problem I: Consider the configuration in Figure 11.11, where $W(s)$ is a stable proper weight, $\mathbf{G}(s)$ is a stable multilinear interval family of systems, and ΔP is any H_∞ perturbation that satisfies $\|\Delta P\| < \alpha$. Find necessary and sufficient conditions for stability of the family of closed loop systems.

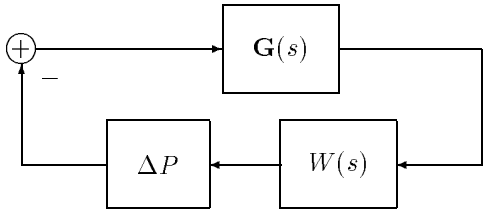

Figure 11.11.

Problem II: Consider the feedback configuration in Figure 11.12, where $W(s)$ is a stable proper weight, ΔP is any H_∞ perturbation that satisfies $\|\Delta P\| < \alpha$, and $C(s)$ is a controller that simultaneously stabilizes every element in the set $\mathbf{G}(s)$. Find necessary and sufficient conditions for stability of the family of closed loop systems.

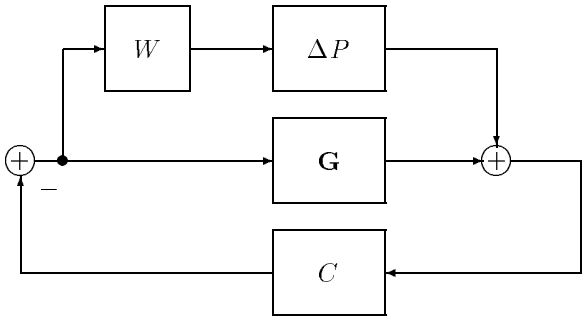

Figure 11.12.

The above problems are generalized versions of standard H_∞ robust stability problems where a fixed plant is considered. Here, the worst case solution is sought over the parameter set $\mathbf{\Pi} \times \mathbf{\Lambda}$. As in the case treated in Chapter 9 (linear case), we solve this problem by using the Small Gain Theorem and determining the worst case over the uncertainty set. The solution is accomplished by showing that the H_∞ norms in question attain their supremum value over the extremal set of transfer functions $\mathbf{G}_{\mathrm{E}}(s) \subset \mathbf{G}(s)$ defined in (11.31). We can now state the main result of this section.

Theorem 11.10 (Unstructured Stability Margins)

1) The configuration of (Figure 11.11) will be stable if and only if α satisfies

$$\alpha \leq \frac{1}{\sup_{g \in \mathbf{G}_{\mathrm{E}}} \|Wg\|_\infty} := \alpha_o^*.$$

2) The configuration of Problem II (Figure 11.12) will be stable if and only if α satisfies

$$\alpha \leq \frac{1}{\sup_{g \in \mathbf{G}_{\mathrm{E}}} \|WC(1+gC)^{-1}\|_\infty} := \alpha_c^*.$$

The proof of this theorem follows from the boundary properties proved in the last section. To state this in more detail, we use the following lemma.

Lemma 11.2 (Extremal H_∞ Properties)

$$\textit{Problem I}: \quad \sup_{g \in \mathbf{G}} \|Wg\|_\infty = \sup_{g \in \mathbf{G}_{\mathrm{E}}} \|Wg\|_\infty,$$

$$\textit{Problem II}: \quad \sup_{g \in \mathbf{G}} \|WC(1+gC)^{-1}\|_\infty = \sup_{g \in \mathbf{G}_{\mathrm{E}}} \|WC(1+gC)^{-1}\|_\infty.$$

Proof. We first consider the following:

$$\begin{aligned}
\sup_{g \in \mathbf{G}_{\mathrm{E}}} \|g\|_\infty &= \sup \{|c| : 0 = c\delta(j\omega, \mathbf{p}) + \gamma(j\omega, \mathbf{l}),\ \mathbf{p} \in \mathbf{\Pi},\ \mathbf{l} \in \mathbf{\Lambda},\ \omega \in [-\infty, +\infty]\} \\
&= \sup \{|c| : 0 = c\delta(j\omega, \mathbf{p}) + \gamma(j\omega, \mathbf{l}) \ , \\
&\qquad (\mathbf{p}, \mathbf{l}) \in (\mathbf{\Pi}_{\mathrm{E}} \times \mathbf{K}(\mathbf{\Lambda})) \cup (\mathbf{K}(\mathbf{\Pi}) \times \mathbf{\Lambda}_{\mathrm{E}}),\ \ \omega \in [-\infty, +\infty]\} \\
&= \sup_{g \in \mathbf{G}_{\mathrm{E}}} \|g\|_\infty.
\end{aligned}$$

Using arguments identical to the above, we conclude that

$$\sup_{g \in \mathbf{G}} \|Wg\|_\infty = \sup_{g \in \mathbf{G}_{\mathrm{E}}} \|Wg\|_\infty,$$

$$\sup_{g \in \mathbf{G}} \|WC(1+gC)^{-1}\|_\infty = \sup_{g \in \mathbf{G}_{\mathrm{E}}} \|WC(1+gC)^{-1}\|_\infty.$$

♣

Proof of Theorem 11.10 Consider the configuration of Figure 11.11. From the Small Gain Theorem the perturbed system is stable if and only if

$$\alpha \leq \frac{1}{\sup_{g \in \mathbf{G}} \|Wg\|_\infty} := \alpha_o^*.$$

From the Lemma 11.2, it follows that $\mathbf{G}$ can be replaced by $\mathbf{G}_{\mathrm{E}}$. A similar argument works for the configuration of Figure 11.12. ♣

Remark 11.3. The quantities α_o^* and α_c^* serve as unstructured H_∞ stability margins for the respective open and closed loop parametrized systems treated in Problems I and II.

Remark 11.4. In practice we can further replace $\mathbf{G}_{\mathrm{E}}(s)$ by the image set overbounding polytopic family $\bar{\mathbf{G}}_{\mathrm{E}}(s)$, and obtain lower bounds on these margins from $\bar{\mathbf{G}}_{\mathrm{E}}(s)$. We can also obtain upper bounds on these margins from the set of Kharitonov vertex systems of the family. Furthermore, the extremal results stated above also hold for any LFT of $\mathbf{G}(s)$.

11.6 NONLINEAR SECTOR BOUNDED STABILITY MARGIN

We now consider the effect of nonlinear perturbations on the multilinear interval family $\mathbf{G}(s)$ defined in the last section (see (11.30)). The nonlinear perturbations will consist of all possible nonlinear gains lying in a sector $[0, k]$. In other words, we consider the configurations in Figures 11.13 and 11.14.

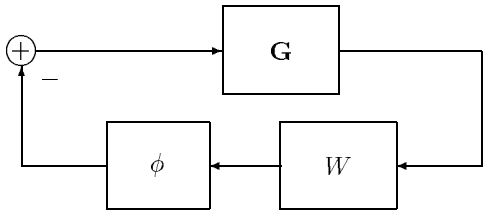

Figure 11.13.

The gain block ϕ consists of all nonlinear time-varying gains $\phi(t, \sigma)$ satisfying

$$\phi(t, 0) = 0 \quad \text{for all } t \geq 0 \qquad \text{and} \qquad 0 \leq \sigma\phi(t, \sigma) \leq k\sigma^2.$$

This implies that $\phi(t, \sigma)$ is bounded by the lines $\phi = 0$ and $\phi = k\sigma$. Such nonlinearities are said to belong to a sector $[0, k]$. $G(s)$ will be assumed to lie in the multilinear interval family $\mathbf{G}(s)$. The problem is to determine the largest size of the sector k for which robust stability is guaranteed. This is the multilinear version

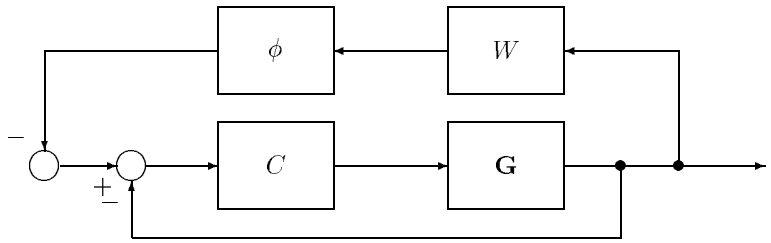

Figure 11.14.

of the robust Lur'e problem treated in Chapter 9. As before, the solution depends on the *strict positive realness* (SPR) properties of the family in question. First we have the following.

Lemma 11.3 (Extremal SPR Properties)

1) Let $\mathbf{G}(s)$ *be the multilinear interval family defined in (11.30) and assume that* $\mathbf{G}(s)$ *is stable. Then*

$$\inf_{G\in\mathbf{G}}\inf_{\omega\in\mathbf{R}}\mathrm{Re}(W(j\omega)G(j\omega)) = \inf_{G\in\mathbf{G}_{\mathrm{E}}}\inf_{\omega\in\mathbf{R}}\mathrm{Re}(W(j\omega)G(j\omega)).$$

2) If $C(s)$ *is a controller that stabilizes the entire family* $\mathbf{G}(s)$*, then*

$$\inf_{G\in\mathbf{G}}\inf_{\omega\in\mathbf{R}}\mathrm{Re}\left(W(j\omega)C(j\omega)G(j\omega)(1+C(j\omega)G(j\omega))^{-1}\right) = \inf_{G\in\mathbf{G}_{\mathrm{E}}}\inf_{\omega\in\mathbf{R}}\mathrm{Re}\left(W(j\omega)C(j\omega)G(j\omega)(1+C(j\omega)G(j\omega))^{-1}\right).$$

The proof of this lemma immediately follows from the boundary property given in Theorem 11.7.

Theorem 11.11 (Nonlinear Stability margin)

1) Let $k^* \geq 0$ *be defined by:*

$$\sup\left\{k \;:\; \frac{1}{k} + \inf_{G\in\mathbf{G}_{\mathrm{E}}}\inf_{\omega\in\mathbf{R}}\mathrm{Re}(W(j\omega)G(j\omega)) > 0\right\}$$

then the closed loop system in Figure 11.13 is absolutely stable for all nonlinear gains ϕ *lying in the sector* $[0, k^*]$*.*

2) Let $k^* \geq 0$ *be defined by:*

$$\sup\left\{k \;:\; \frac{1}{k} + \inf_{G\in\mathbf{G}_{\mathrm{E}}}\inf_{\omega\in\mathbf{R}}\mathrm{Re}\left(W(j\omega)C(j\omega)G(j\omega)(1+C(j\omega)G(j\omega))^{-1}\right) > 0\right\}$$

for the controller C, then the closed loop system in Figure 11.14 is absolutely stable for all nonlinear gains ϕ lying in the sector $[0, k^*]$.

Proof. From standard results on the Lur'e problem, stability is preserved for all k satisfying

$$\frac{1}{k} + \inf_{G \in \mathbf{G}} \inf_{\omega \in \mathbf{R}} \mathrm{Re}(W(j\omega)G(j\omega)) > 0.$$

By Lemma 11.3 we may replace $\mathbf{G}(j\omega)$ by $\mathbf{G}_{\mathrm{E}}(j\omega)$ in the above inequality. This proves 1). The proof of 2) is similar. ♣

Example 11.5. (Stability Sector for Multilinear Interval Systems) Consider the system used in Example 11.1. We plot the frequency domain image of the closed loop system transfer function

$$\mathbf{M}(s) := \left\{ \frac{F(s)G(s)}{1 + F(s)G(s)} : G(s) \in \mathbf{G}_{\mathrm{E}}(s) \right\}.$$

Figure 11.15 shows that the nonlinear sector is given by $\frac{1}{k} = 20.5012$.

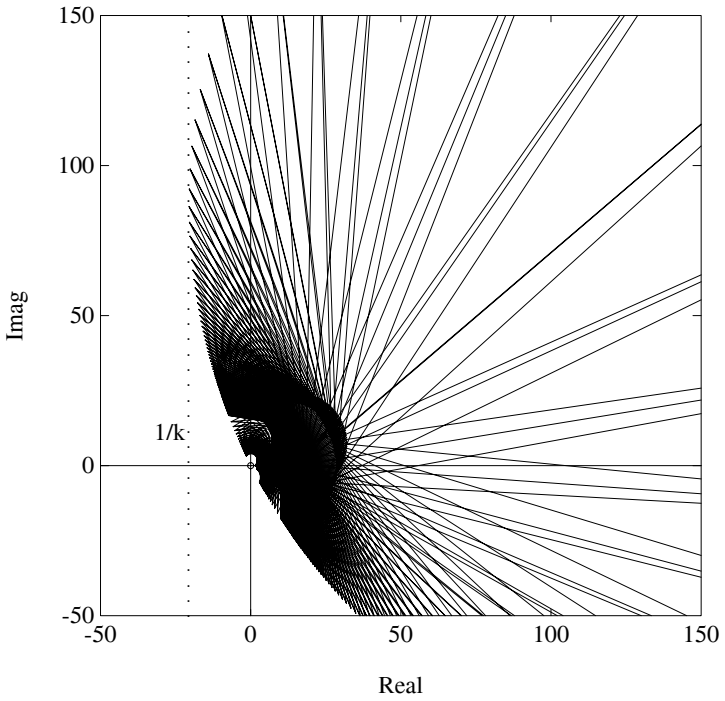

Figure 11.15. Frequency domain image of $\mathbf{M}(j\omega)$ (Example 11.5)

11.7 INTERVAL PLANTS AND DIAGONAL REPRESENTATION OF PERTURBATIONS

In the robust control literature it has become customary to represent system perturbations in a signal flow diagram where the perturbations are "pulled" out and displayed in a feedback matrix $\mathbf{\Delta}$ with independent diagonal or block-diagonal entries Δ_i as shown below in Figure 11.16.

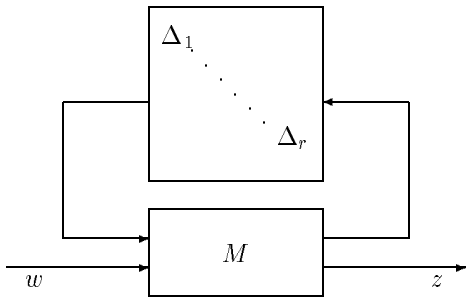

Figure 11.16. System with uncertainties represented in feedback form

$M(s)$ is a suitably defined interconnection transfer function matrix of appropriate size and Δ is a block diagonal matrix containing all the perturbations affecting the system dynamics. In general this would include real parametric uncertainty as well as norm-bounded uncertainty blocks with the latter representing either actual unmodelled dynamics or fictitious performance blocks. The popularity of this representation is due to the fact that almost all types of uncertainties including parametric and unstructured uncertainties can be accurately and explicitly represented in this framework. Moreover, the feedback representation allows us to use the Small Gain formulation and thus convert robust performance problems into robust stability problems.

Although this formulation does not add anything to the the rich structure of interval systems already developed, it is nevertheless instructive to interpret the solution given by the Generalized Kharitonov Theorem in the linear and multilinear cases in this framework. We begin in the next subsection with the diagonal representation of a single interval system. This is subsequently extended to the case of multiple interval systems and multiple norm-bounded perturbation blocks. This type of mixed perturbation problem arises in systems with several performance specifications. We show how the boundary properties of the extremal systems $\mathbf{G}_{\mathrm{E}}(s)$ established in the GKT play a role in the solution of these problems.

11.7.1 Diagonal Feedback Representation of an Interval System

Let $\mathbf{G}(s)$ be a interval plant

$$\mathbf{G}(s) = \left\{ \frac{N(s)}{D(s)} \ : \ (N(s) \times D(s) \in (\mathbf{N}(s) \times \mathbf{D}(s)) \right\} \tag{11.45}$$

where $\mathbf{N}(s)$ and $\mathbf{D}(s)$ are interval polynomial families. Referring to the notation defined in Chapter 5, the four Kharitonov polynomials associated with the interval polynomial $\mathbf{D}(s)$ can be written as follows:

$$\begin{aligned} K_D^1(s) &= D_{\min}^{\text{even}}(s) + D_{\min}^{\text{odd}}(s) \\ K_D^2(s) &= D_{\min}^{\text{even}}(s) + D_{\max}^{\text{odd}}(s) \\ K_D^3(s) &= D_{\max}^{\text{even}}(s) + D_{\min}^{\text{odd}}(s) \\ K_D^4(s) &= D_{\max}^{\text{even}}(s) + D_{\max}^{\text{odd}}(s). \end{aligned} \tag{11.46}$$

We know that, as far as frequency domain properties at $s = j\omega$ are concerned, the interval polynomial $\mathbf{D}(s)$ can be replaced by the following reduced 2-parameter family:

$$\mathbf{D}_R(s) = \left\{ D(s) \ : \ D^0(s) + \lambda_1 D_e(s) + \lambda_2 D_o(s) \ \ \lambda_i \in [-1, 1] \right\} \tag{11.47}$$

where

$$\begin{aligned} D_e(s) &= \frac{1}{2} \left(D_{\max}^{\text{even}}(s) - D_{\min}^{\text{even}}(s) \right) \\ D_o(s) &= \frac{1}{2} \left(D_{\max}^{\text{odd}}(s) - D_{\min}^{\text{odd}}(s) \right) \end{aligned}$$

and

$$D^0(s) = \frac{1}{2} \left[D_{\max}^{\text{even}}(s) + D_{\min}^{\text{even}}(s) + D_{\max}^{\text{odd}}(s) + D_{\min}^{\text{odd}}(s) \right]$$

is the *nominal* polynomial. Similarly $\mathbf{N}(s)$ can be replaced by:

$$\mathbf{N}_R(s) = \left\{ N(s) \ : \ N^0(s) + \lambda_3 N_e(s) + \lambda_4 N_o(s), \quad \lambda_i \in [-1, 1] \right\}. \tag{11.48}$$

It is clear from the above that an interval plant is completely characterized in the frequency domain by the 4-parameter family $\mathbf{G}_{\mathrm{R}}(s)$:

$$\mathbf{G}_{\mathrm{R}}(s) = \left\{ \frac{N(s)}{D(s)} \ : \ (N(s) \times D(s)) \in (\mathbf{N}_{\mathrm{R}}(s) \times \mathbf{D}_{\mathrm{R}}(s)) \right\}. \tag{11.49}$$

This is essentially what we proved in the first step of the proof of GKT given in Chapter 7. In the second step we proved further that it suffices to test stability of the extremal set $\mathbf{G}_{\mathrm{E}}(s)$. The polynomial set $\mathbf{G}_{\mathrm{K}}(s)$ corresponds to the vertices of the 4-dimensional box representing $\mathbf{G}_{\mathrm{R}}(s)$ while the 32 segments $\mathbf{G}_{\mathrm{E}}(s)$, correspond to the exposed edges of the same box.

Now write $y(s) = G(s)u(s)$,

$$y(s) = \frac{N^0(s) + \lambda_3 N_e(s) + \lambda_4 N_o(s)}{D^0(s) + \lambda_1 D_e(s) + \lambda_2 D_o(s)} u(s).$$

This may be rewritten as follows:

$$\begin{aligned} y(s) = \left[D^0(s)\right]^{-1} \big\{ &\left(N^0(s) + \lambda_3 N_e(s) + \lambda_4 N_o(s)\right) u(s) \\ &- \left(\lambda_1 D_e(s) + \lambda_2 D_o(s)\right) y(s) \big\} \end{aligned} \tag{11.50}$$

or, suppressing s, as

$$\begin{aligned} y = \left[(D^0)^{-1} N^0 + \lambda_3 (D^0)^{-1} N_e + \lambda_4 (D^0)^{-1} N_o\right] u \\ - \left[\lambda_1 (D^0)^{-1} D_e + \lambda_2 (D^0)^{-1} D_o\right] y. \end{aligned} \tag{11.51}$$

Corresponding to (11.51), we have the block diagram shown in Figure 11.17.

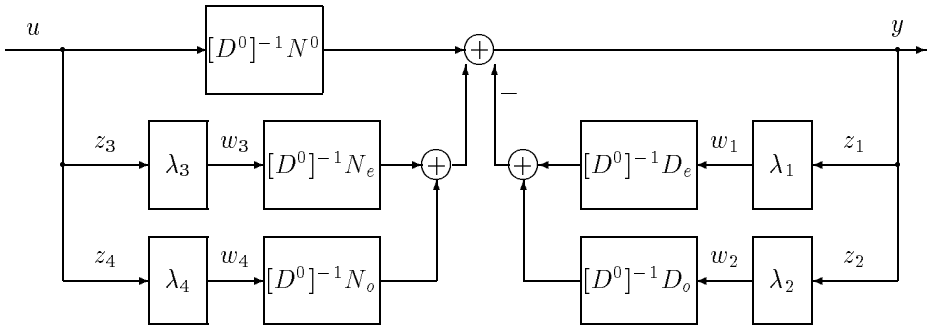

Figure 11.17. Four parameter structure

This input-output relation may be written as follows:

$$\begin{bmatrix} z_1 \\ z_2 \\ z_3 \\ z_4 \\ y \end{bmatrix} = (D^0)^{-1} \begin{bmatrix} -D_e & -D_o & N_e & N_o & N^0 \\ -D_e & -D_o & N_e & N_o & N^0 \\ 0 & 0 & 0 & 0 & D^0 \\ 0 & 0 & 0 & 0 & D^0 \\ -D_e & -D_o & N_e & N_o & N^0 \end{bmatrix} \begin{bmatrix} w_1 \\ w_2 \\ w_3 \\ w_4 \\ u \end{bmatrix} \tag{11.52}$$

with

$$w_i = \lambda_i z_i, \quad i = 1, 2, 3, 4. \tag{11.53}$$

Let $z := [z_1, z_2, z_3, z_4]^T$ and $w := [w_1, w_2, w_3, w_4]^T$. The above equations can then be rewritten as

$$z(s) = M_{11}(s)w(s) + M_{12}(s)u(s)$$

$$y(s) = M_{21}(s)w(s) + M_{22}(s)u(s)$$
$$w(s) = \Delta z(s).$$

where

$$M(s) = \begin{bmatrix} M_{11}(s) \vdots M_{12}(s) \\ \cdots \quad \cdots \\ M_{21}(s) \vdots M_{22}(s) \end{bmatrix}$$

$$= \begin{bmatrix} -[D^0]^{-1}D_e & -[D^0]^{-1}D_o & [D^0]^{-1}N_e & [D^0]^{-1}N_o & \vdots & [D^0]^{-1}N^0 \\ -[D^0]^{-1}D_e & -[D^0]^{-1}D_o & [D^0]^{-1}N_e & [D^0]^{-1}N_o & \vdots & [D^0]^{-1}N^0 \\ 0 & 0 & 0 & 0 & \vdots & 1 \\ 0 & 0 & 0 & 0 & \vdots & 1 \\ \cdots\cdots & \cdots\cdots & \cdots\cdots & \cdots\cdots & & \cdots\cdots \\ -[D^0]^{-1}D_e & -[D^0]^{-1}D_o & [D^0]^{-1}N_e & [D^0]^{-1}N_o & \vdots & [D^0]^{-1}N^0 \end{bmatrix} \quad (11.54)$$

and

$$\Delta = \Delta^R := \begin{bmatrix} \lambda_1 & & & \\ & \lambda_2 & & \\ & & \lambda_3 & \\ & & & \lambda_4 \end{bmatrix}.$$

Consequently, we have the configuration shown in Figure 11.18.

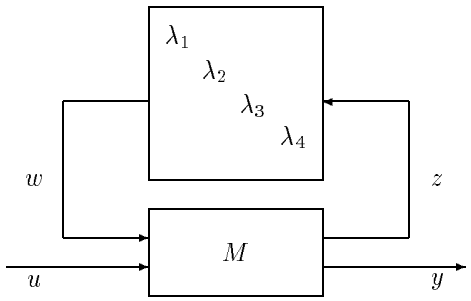

Figure 11.18. 4-parameter feedback representation of an interval system

The result established in Step 2 of the proof of GKT given in Chapter 7 tells us that robust stability of the four parameter feedback structure given in Figure 11.18 is further equivalent to that of a reduced set of one-parameter extremal feedback structures in which each structure contains a single perturbation block. In Figure 11.19 we display a typical such extremal system structure where λ_1 is the only perturbation block and the remaining λ's are set to the vertex values $+1$ or -1.

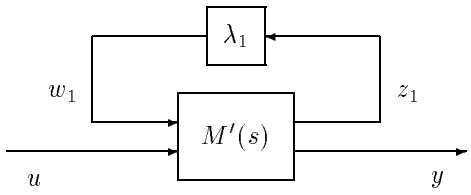

Figure 11.19. A typical element of the extremal set $\mathbf{G}_{\mathrm{E}}(s)$

This is denoted in the equations by writing $\lambda_2 = \lambda_2^*$, $\lambda_3 = \lambda_3^*$ and $\lambda_4 = \lambda_4^*$. The system equations assume the form

$$\begin{bmatrix} z_1 \\ y \end{bmatrix} = \underbrace{\begin{bmatrix} M'_{11}(s) & M'_{12}(s) \\ M'_{21}(s) & M'_{22}(s) \end{bmatrix}}_{M'(s)} \begin{bmatrix} w_1 \\ u \end{bmatrix} \tag{11.55}$$

with

$$w_1 = \lambda_1 z_1$$

where

$$M'_{11}(s) = M'_{21}(s) = (1 + \lambda_2^*[D^0]^{-1}D_o)^{-1}[D^0]^{-1}D_e$$
$$M'_{21}(s) = M'_{22}(s) = (1 + \lambda_2^*[D^0]^{-1}D_o)^{-1}[D^0]^{-1}N^0 + \lambda_3^*[D^0]^{-1}N_e + \lambda_4^*[D^0]^{-1}N_o.$$

The interval plant $\mathbf{G}(s)$ can *always* be replaced by the above set of one-parameter structures $\mathbf{G}_{\mathrm{E}}(s)$ regardless of the rest of the feedback system. If the intervals in which the parameters vary are not fixed *apriori* one can also determine their maximum permissible excursion using the same framework. The only difference in this case is that the Kharitonov polynomials, and therefore the system M' defined from them, have parameters which depend on the dilation parameter ϵ as shown below in Figure 11.20.

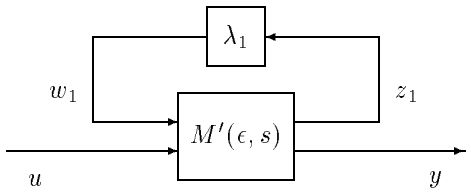

Figure 11.20. An element of $\mathbf{G}_{\mathrm{E}}(\epsilon, s)$

The limiting value ϵ^* of ϵ is determined as the smallest value of ϵ for which the control system containing one of the one parameter structures representing $\mathbf{G}_{\mathrm{E}}(\epsilon, s)$ acquires a pole on the imaginary axis. Thus ϵ^* can be found using several methods which include the Segment Lemma and the Bounded Phase Conditions of Chapter 2. Of course, by restricting attention to the class of controllers which satisfy the vertex conditions given in GKT we get further simplification in that *all* the λ's can be frozen at vertices, and ϵ^* can be found from the vertex systems.

The above discussion may be summarized by stating that if $\mathbf{G}(s)$ is an interval plant contained within a control system structure, we can always replace it with the set of one-parameter extremal systems $\mathbf{G}_{\mathrm{E}}(s)$ for the purposes of determining worst case performance and stability margins and for carrying out worst case frequency response analysis. This observation holds also for linear interval systems and polytopic systems as defined in Chapter 8. In the case of multilinear interval systems we can again replace the plant set $\mathbf{G}(s)$ by the corresponding set of extremal systems $\mathbf{G}_{\mathrm{E}}(s)$ which now consist of a set reduced dimensional multilinear systems in terms of the interval parameters λ_i. This can in turn be replaced by a polytopic family using the Mapping Theorem. Finally, an extremal one-parameter family can be constructed for this polytopic system as shown in this chapter.

11.7.2 Interval Plant with H_∞ Norm-Bounded Uncertainty

Now let us consider the mixed uncertainty system in Figure 11.21.

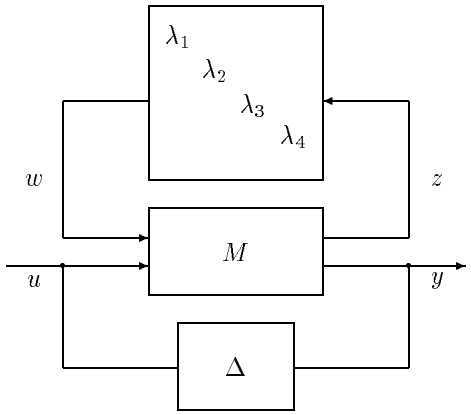

Figure 11.21. 4-parameter representation of interval system with unstructured uncertainty

It consists of an interval plant with an unstructured perturbation block Δ lying in a H_∞ ball of specified radius. As before, the interval plant can be represented in terms of four feedback parameters around a suitable interconnection transfer matrix $M(s)$. We can now represent all the perturbations, parametric as well as unstructured, in feedback form around a suitably defined system $P(s)$. Thus, we have the structure shown in Figure 11.22 with an appropriate $P(s)$.

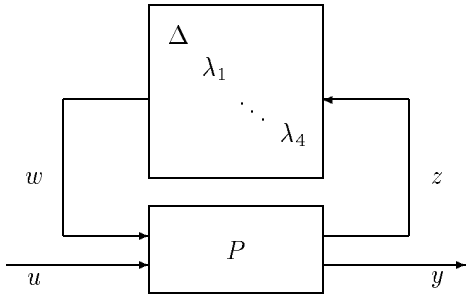

Figure 11.22. Feedback representation of mixed uncertainties

Moreover, by using the result of Chapter 9 on extremal values of H_∞ norms, this four-parameter system can be reduced to the extremal set of single parameter uncertainty problems. A typical element of this extremal set is shown in Figure 11.23 with an appropriate $P'(s)$.

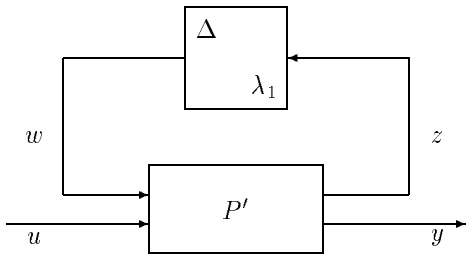

Figure 11.23. A typical element of the extremal set of systems

By eliminating the feedback loop associated with λ this can also be represented as the structure shown in Figure 11.24.

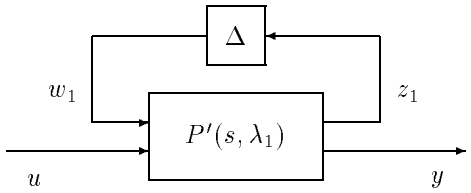

Figure 11.24. Equivalent representation of an extremal system

11.7.3 Multiple Interval Systems and Unstructured Blocks

Let us now consider the general configuration given in Figure 11.25.

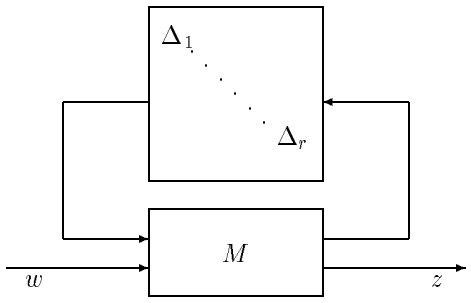

Figure 11.25. System with uncertainties represented in feedback form

$M(s)$ is an interconnection transfer function matrix of suitable dimensions and $\Delta^U(s)$ is a diagonal matrix containing all the unstructured system perturbations. The unstructured perturbations can be considered by introducing the class of perturbations $\mathbf{D}^u(r)$ defined as

$$\mathbf{D}^u(r) = \left\{ \Delta^U = \begin{bmatrix} \Delta_1 & & \\ & \ddots & \\ & & \Delta_r \end{bmatrix} \; : \; \Delta_i \in \mathbf{\Delta}_1 \right\} \tag{11.56}$$

where $\mathbf{\Delta}_1$ is a ball in the space of H_∞ real rational functions, denoted by RH_∞, with radius 1

$$\mathbf{\Delta}_1 = \{\Delta \; : \; \Delta \in RH_\infty, \;\; \|\Delta\|_\infty \leq 1\} .$$

Parametric perturbations or uncertainty can be modeled by letting interval transfer functions represent each physically distinct subsystem. These individual systems can then be "pulled out" and represented in feedback form as described earlier. The

result of doing this is the general representation of the system shown in Figure 11.26.

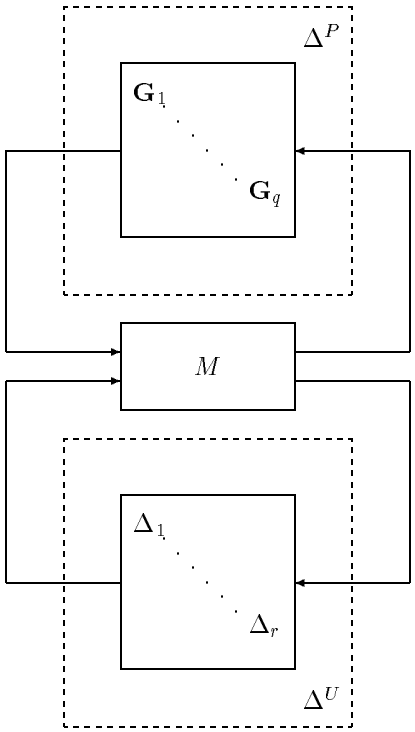

Figure 11.26. Feedback representation of multiple interval plants and unstructured uncertainties

In this representation, the Δ^U block represents multiple norm-bounded uncertainties, and the Δ^P block accounts for parameter perturbations modeled as the set of independent interval systems $\mathbf{G}^i(s)$ arranged in diagonal form:

$$\mathbf{D}^G(q) = \left\{ \begin{bmatrix} G_1 & & \\ & \ddots & \\ & & G_q \end{bmatrix} \; : \; G_i \in \mathbf{G}^i \right\}. \tag{11.57}$$

From the discussion of the last subsection we can immediately replace each interval system by a four-parameter set. Further we can also replace each interval system

$\mathbf{G}^i(s)$ by the corresponding extremal set $\mathbf{G}^i_{\mathrm{E}}$:

$$\mathbf{D}^G_{\mathrm{E}}(q) = \left\{ \begin{bmatrix} G_1 & & \\ & \ddots & \\ & & G_q \end{bmatrix} \; : \; G_i \in \mathbf{G}^i_{\mathrm{E}} \right\}. \tag{11.58}$$

For carrying out frequency domain analysis, the system in Figure 11.26 can therefore be replaced by Figure 11.27 where Δ^{UP} belongs to the mixed complex-real perturbation class $\mathbf{D}^{UP}$ defined as

$$\mathbf{D}^{UP}(r;4q) = \left\{ \begin{bmatrix} \Delta^U & & & \\ & \lambda_1 & & \\ & & \ddots & \\ & & & \lambda_{4q} \end{bmatrix} \right\}. \tag{11.59}$$

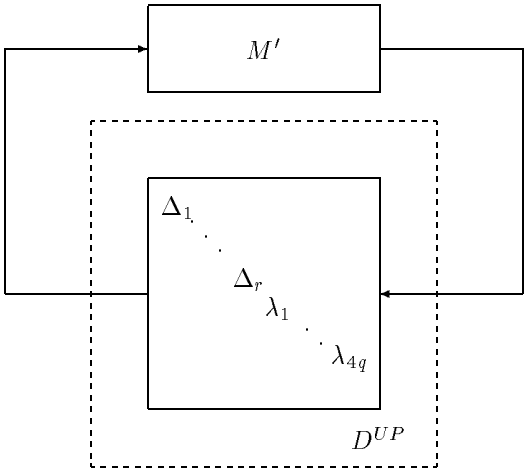

Figure 11.27. Feedback representation of mixed complex-real block diagonal uncertainties

This representation can be used to formulate a variety of robust stability and performance problems. We illustrate this by considering two specific examples.

Example 11.6. Consider the control system shown in Figure 11.28. In this system there are two independent subsystems containing parametric uncertainty which are modelled by the interval systems $G_1(s) \in \mathbf{G}^1(s)$ and $G_2(s) \in \mathbf{G}^2(s)$. Unstructured perturbations are represented by the block Δ_1, and appropriate scalings have been introduced to allow Δ_1 to belong to $\mathbf{\Delta}_1$, the H_∞ ball of radius unity. The specifications on the system performance are stated as the following requirements:

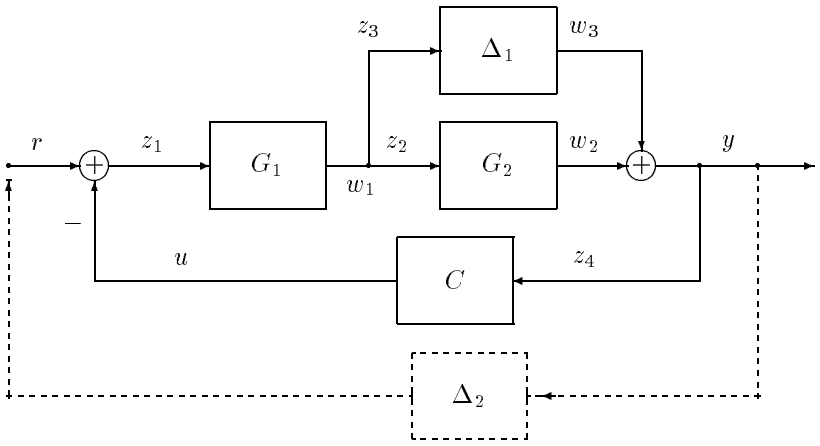

Figure 11.28. Robust performance problem (Example 11.6)

1) *Robust Stability* The system must be stable for all $G_1(s) \in \mathbf{G}^1(s)$, $G_2(s) \in \mathbf{G}^2(s)$, $\Delta_1 \in \mathbf{\Delta}_1$ and

2) *Robust Performance* The worst case H_∞ norm of the closed loop transfer function be bounded by unity:

$$\sup_{\mathbf{G}^1, \mathbf{G}^2, \mathbf{\Delta}_1} \|T_{ry}(G_1, G_2, \Delta_1)\|_\infty < 1,$$

where T_{ry} is the transfer function from r to y.

This problem can be cast in the framework developed above, and treated as a robust stability problem by introducing a fictitious performance block $\Delta_2 \in \mathbf{\Delta}_1$ connected between r and y as shown in Figure 11.28. The equations describing the system in Figure 11.28 are

$$\begin{bmatrix} z_1 \\ z_2 \\ z_3 \\ z_4 \\ y \end{bmatrix} = \begin{bmatrix} 0 & 0 & 0 & 1 & -1 \\ 1 & 0 & 0 & 0 & 0 \\ 1 & 0 & 0 & 0 & 0 \\ 0 & 1 & 1 & 0 & 0 \\ 0 & 1 & 1 & 0 & 0 \end{bmatrix} \begin{bmatrix} w_1 \\ w_2 \\ w_3 \\ r \\ u \end{bmatrix}$$

$$\begin{bmatrix} w_1 \\ w_2 \\ w_3 \\ r \\ u \end{bmatrix} = \begin{bmatrix} G_1 & 0 & 0 & 0 & 0 \\ 0 & G_2 & 0 & 0 & 0 \\ 0 & 0 & \Delta_1 & 0 & 0 \\ 0 & 0 & & \Delta_2 & 0 \\ 0 & 0 & 0 & 0 & C \end{bmatrix} \begin{bmatrix} z_1 \\ z_2 \\ z_3 \\ z_4 \\ y \end{bmatrix}.$$

The "feedback" perturbations belong to the class

$$\mathbf{D}^G(2) = \left\{ \begin{bmatrix} G_1 & \\ & G_2 \end{bmatrix} \ : \ G_1 \in \mathbf{G}^1, G_2 \in \mathbf{G}^2 \right\}$$

$$\mathbf{D}^U(2) = \left\{ \begin{bmatrix} \Delta_1 & \\ & \Delta_2 \end{bmatrix} \ : \ \Delta_1, \Delta_2 \in \mathbf{\Delta}_1 \right\}$$

and the interconnection matrix is

$$M = \begin{bmatrix} 0 & 0 & 0 & 1 & -1 \\ 1 & 0 & 0 & 0 & 0 \\ 1 & 0 & 0 & 0 & 0 \\ 0 & 1 & 1 & 0 & 0 \\ 0 & 1 & 1 & 0 & 0 \end{bmatrix}.$$

Example 11.7. We consider the system in Figure 11.29.

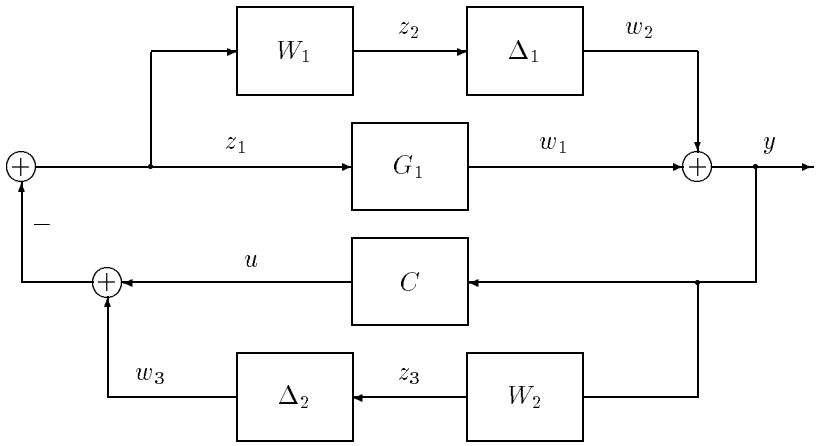

Figure 11.29. Robust stability problem (Example 11.7)

Parameter uncertainty is represented by the interval system $G_1(s) \in \mathbf{G}^1(s)$ and unstructured uncertainty consists of two independent blocks $\Delta_1, \Delta_2 \in \mathbf{\Delta}_1$. $W_1(s)$ and $W_2(s)$ represent frequency weightings and consist of fixed stable, proper minimum phase transfer functions. The system equations are

$$\begin{bmatrix} z_1 \\ z_2 \\ z_3 \\ y \end{bmatrix} = \begin{bmatrix} 0 & 0 & -1 & -1 \\ 0 & 0 & -W_1 & -W_1 \\ W_2 & W_2 & 0 & 0 \\ 1 & 1 & 0 & 0 \end{bmatrix} \begin{bmatrix} w_1 \\ w_2 \\ w_3 \\ u \end{bmatrix}$$

$$\begin{bmatrix} w_1 \\ w_2 \\ w_3 \\ u \end{bmatrix} = \begin{bmatrix} G_1 & 0 & 0 & 0 \\ 0 & \Delta_1 & 0 & 0 \\ 0 & 0 & \Delta_2 & 0 \\ 0 & 0 & 0 & C \end{bmatrix} \begin{bmatrix} z_1 \\ z_2 \\ z_3 \\ y \end{bmatrix}.$$

This configuration fits the general structure developed above with the "feedback" perturbation classes being

$$\mathbf{D}^G(1) = \left\{ G_1 \ : \ G_1 \in \mathbf{G}^1 \right\}$$

and

$$\mathbf{D}^U(2) = \left\{ \begin{bmatrix} \Delta_1 & \\ & \Delta_2 \end{bmatrix} \ : \ \Delta_1, \Delta_2 \in \mathbf{\Delta}_1 \right\}$$

and the interconnection matrix

$$M = \begin{bmatrix} 0 & 0 & -1 & -1 \\ 0 & 0 & -W_1 & -W_1 \\ W_2 & W_2 & 0 & 0 \\ 1 & 1 & 0 & 0 \end{bmatrix}.$$

11.7.4 Extremal Properties

We have shown that parameter uncertainty can be modelled by interval systems and that both parametric and norm-bounded uncertainty can be represented in feedback form. Moreover, each interval system can be replaced, as far as worst case frequency domain analysis is concerned, by the corresponding reduced 4-parameter family.

Let us now consider the system in Figure 11.26. Suppose that a stabilizing controller for the nominal system has been connected between y and u. The controller is stabilizing when the feedback perturbation is zero. Let $M(s)$ denote the interconnection matrix with the controller attached. We now wish to determine if the control system is robustly stable under the feedback perturbations given. This is a real-complex mixed perturbation robust stability problem with the diagonal "feedback" perturbation matrix (see Figure 11.27)

$$\mathbf{D}^{UP} = \left\{ D^{UP} = \begin{bmatrix} \Delta_1 & & & & & \\ & \ddots & & & & \\ & & \Delta_r & & & \\ & & & \lambda_1 & & \\ & & & & \ddots & \\ & & & & & \lambda_{4m} \end{bmatrix} \ : \ \Delta_1 \in \mathbf{\Delta}_1, \ |\lambda_i| \leq 1 \right\}.$$

We make the standing assumption that the McMillan degree of the system remains invariant under the perturbations. The first observation we can make is obvious.

Theorem 11.12 *The system in Figure 11.26 is Hurwitz stable for all* $D^P \in \mathbf{D}^G(m)$ *and all* $D^u \in \mathbf{D}^U(r)$ *if and only if the system in Figure 11.27 is Hurwitz stable for all* $D^{UP} \in \mathbf{D}^{UP}$.

The above theorem actually applies more generally. For instance a more general formulation could allow for repeated interval system blocks.

As a further simplification in the above result, we can replace each interval system $\mathbf{G}^i(s)$ by the corresponding set of extremal systems $\mathbf{G}^i_{\mathrm{E}}(s)$. This corresponds to replacing each set of 4 λ_i's in Figure 11.27 by their exposed edges.

Theorem 11.13 *The system in Figure 11.26 is Hurwitz stable for all* $D^P \in \mathbf{D}^G(m)$ *and all* $D^u \in \mathbf{D}^U(r)$ *if and only if the system in Figure 11.27 is Hurwitz stable for all* $D_P \in \mathbf{D}^G_{\mathrm{E}}(m)$ *and all* $D^u \in \mathbf{D}^U(r)$.

Proof. The proof of this result follows immediately from the fact that the characteristic equation of the system in Figure 11.27 is a multilinear function of the interval systems $\mathbf{G}^i_{\mathrm{E}}(s)$. Therefore, by the result derived in Theorem 11.8, we can replace each interval system $\mathbf{G}^i(s)$ by the corresponding extremal set $\mathbf{G}^i_{\mathrm{E}}(s)$. ♣

Remark 11.5. The result stated above can be interpreted in terms of the worst case norm-bounded stability margin of the system over the interval parameter uncertainty set. For a prescribed D^P, this stability margin is usually measured as a norm of the smallest destabilizing diagonal perturbation matrix Δ. The norm customarily used is the maximum singular value. The worst case value of this stability margin as D^P ranges over the interval systems can be found by restricting D^P to range over the extremal systems only. This is obviously a tremendous saving in computational effort.

11.8 EXERCISES

11.1 Consider the feedback system with a parallel structure in the forward path as shown in Figure 11.30.

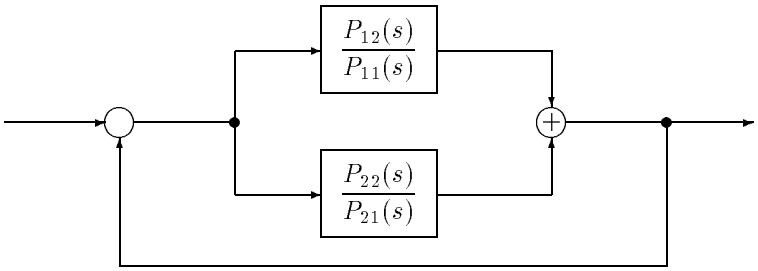

Figure 11.30. Feedback system with parallel structure (Exercise 11.1)

Suppose that

$$P_1(s) = \frac{P_{12}(s)}{P_{11}(s)} = \frac{\alpha_2 s^2 + \alpha_1 s + \alpha_0}{s^2 + \alpha_4 s + \alpha_3}$$
$$P_2(s) = \frac{P_{22}(s)}{P_{21}(s)} = \frac{\beta_2 s^2 + \beta_1 s + \beta_0}{s^2 + \beta_4 s + \beta_3}$$

where the parameters vary as follows:

$$\alpha_i \in [\alpha_i^-, \alpha_i^+], \quad \text{and} \quad \beta_i \in [\beta_i^-, \beta_i^+], \qquad i = 0, 1, 2, 3, 4.$$

a) Use the multilinear GKT (Theorem 11.1) to write down all the manifolds which are necessary to verify the robust Hurwitz stability of the closed loop system.

b) Write down all the manifolds which are necessary to verify the robust stability of the closed loop system with respect to the stability region which is a circle centered at $-\gamma$ with radius r where $\gamma > r > 0$.

c) One may observe that a significant reduction, in terms of the number of manifolds to be checked, is achieved for the case a) over b). Explain the reason.

11.2 Consider the feedback system shown in Figure 11.31.
Let

$$C(s) = \frac{1}{s+1}, \quad P_1(s) = \frac{p_0}{s+q_0}, \quad P_2(s) = \frac{p_1}{s+q_1}$$

with

$$q_0 \in [0.5, 1.5], \quad p_0 \in [0.5, 1.5], \quad q_1 \in [1.5, 2.5], \quad p_1 \in [0.5, 1.5].$$

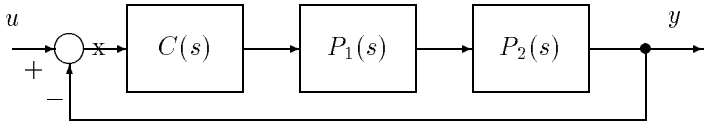

Figure 11.31. Feedback system (Exercise 11.2)

Using the polytopic approximation, plot the Bode magnitude and phase envelopes of the open loop system and estimate from this the guaranteed gain and phase margin of the family.

11.3 For the feedback system given in Exercise 11.2,

a) plot the Nyquist envelope of the closed loop transfer function by using the polytopic approximation,

b) from the plot in a) determine the exact guaranteed gain and phase margin of the system and compare with the estimates obtained in the previous exercise,

c) suppose that a nonlinear feedback gain is connected as shown in Figure 11.32.

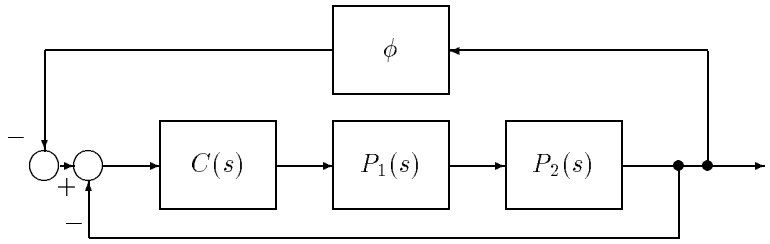

Figure 11.32. Feedback system with nonlinear gain (Exercise 11.3)

Determine the Lur'e sector for which the the closed loop system is robustly absolutely stable.

11.4 Referring to the system given in Exercise 11.2, find the maximum value of M-peak of the closed loop system. What can you say about the minimum value of M-peak?
Hint: The maximum value of M-peak is obtained by selecting the peak value of the upper curve of the magnitude envelope of the closed loop system. However, the peak value of the lower curve does not necessarily serve as the minimum value

of M-peak as it may not correspond to M-peak for some bona fide set of system parameters. It can only be a lower bound on the minimum M-peak.

11.5 Referring to the system in Exercise 11.2, plot the magnitude envelope of the error transfer function and determine the worst case amplitude of the error, with respect to unit amplitude sinusoidal inputs, over the parameter set given.

11.6 Consider the feedback system shown below in Figure 11.33.

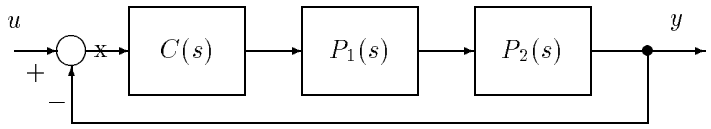

Figure 11.33. Feedback system (Exercise 11.6)

Let

$$C(s) = 2, \quad P_1(s) = \frac{s+\beta_0}{s^2+\beta_1 s+\beta_2}, \quad P_2(s) = -\frac{s+\alpha_0}{s+\alpha_1}$$

with the nominal values of the parameters being

$$\alpha_0^0 = 1.5, \quad \alpha_1^0 = 5, \quad \beta_0^0 = 4, \quad \beta_1^0 = 4.5, \quad \beta_2^0 = 1.5.$$

Determine the maximum parametric stability margin ϵ around these nominal values, i.e.the largest value of ϵ for which the system remains robustly stable for the parameter excursions

$$\alpha_i \in [\alpha_i^0 - \epsilon, \alpha_i^0 + \epsilon], \quad i = 0, 1 \quad \text{and} \quad \beta_j \in [\beta_j^0 - \epsilon, \beta_j^0 + \epsilon], \quad j = 0, 1, 2.$$

11.7 Referring to the system in Exercise 11.6 with ϵ being set to be the stability margin obtained in Exercise 11.6,

a) plot the Nyquist envelope of the open loop multilinear interval system as well as the Nyquist plot of the open loop nominal system,

b) plot the Bode magnitude and phase envelopes of the open loop family of systems as well as the Bode plots of the nominal system.

11.8 In the system of Exercise 11.6, suppose that unstructured uncertainty Δ is introduced as shown in Figure 11.34.
Find the maximum unstructured H_∞ uncertainty that can be tolerated by the system.

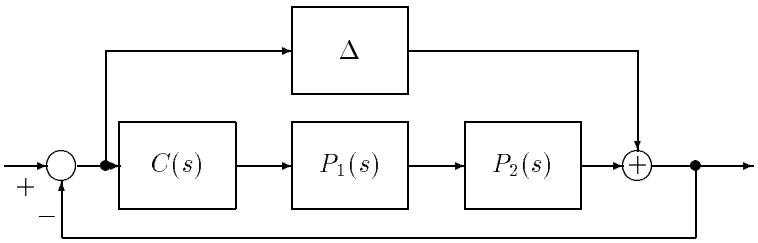

Figure 11.34. Feedback system with unstructured uncertainty (Exercise 11.8)

11.9 Let $C(s)$ be a fixed controller that robustly stabilizes an interval plant $\mathbf{G}(s)$ with extremal set $\mathbf{G}_{\mathrm{E}}(s)$. Define

$$M(s) := \begin{bmatrix} (1+G(s)C(s))^{-1} & (1+G(s)C(s))^{-1} \\ -G(s)C(s)\,(1+G(s)C(s))^{-1} & -G(s)C(s)\,(1+G(s)C(s))^{-1} \end{bmatrix}$$

and let

$$\mathbf{M}(s) := \{M(s) : G(s) \in \mathbf{G}(s)\},$$

and

$$\mathbf{M}_{\mathrm{E}}(s) := \{M(s) : G(s) \in \mathbf{G}_{\mathrm{E}}(s)\}.$$

Consider the perturbation structure $\mathbf{D}(2)$ of all diagonal perturbations of the form $D = \mathrm{diag}\,\{\Delta_1, \Delta_2\}$ where $\|\Delta_i\|_\infty < 1$. Let $M(s)$ be any element in $\mathbf{M}(s)$, and denote by $M(j\omega)$ its evaluation at the $j\omega$-axis. Let $\bar{\sigma}(M)$ denote the maximum singular value of M. We can define $\mu_{\mathbf{D}(2)}(M(j\omega)$ as follows:

$$\frac{1}{\mu_{\mathbf{D}(2)}(M(j\omega))} := \min\{\bar{\sigma}(D) : D \in \mathbf{D}(2), \quad \det(I + M(j\omega)D) = 0\}.$$

Show that

$$\sup_{M\in\mathbf{M}} \sup_{\omega} \mu_{\mathbf{D}(2)}(M(j\omega)) = \sup_{M\in\mathbf{M}_{\mathrm{E}}} \sup_{\omega} \mu_{\mathbf{D}(2)}(M(j\omega)).$$

Hint: Replace Δ_i in $\det(I + M(j\omega)D) = 0$ by complex numbers δ_i and apply the complex version of GKT (Chapter 7).

11.9 NOTES AND REFERENCES

The multilinear version of the Generalized Kharitonov Theorem given here is contained in the papers by Chapellat, Keel, and Bhattacharyya [66] and Chapellat, Dahleh, and Bhattacharyya [65]. The extremal properties with respect to various

margins given in this chapter are described in the paper by Chapellat, Keel, and Bhattacharyya [67]. The result on Hurwitz stability of interval polynomial matrices (Theorem 11.2) is due to Kokame and Mori [150]. The method of constructing the frequency template of a multilinear interval control systems given in Section 11.4.1 is described in Ahmad, Keel and Bhattacharyya [8]. Saeki [199] also obtained a sufficient condition for robust stability of such classes of systems by applying the Mapping Theorem to the Nyquist stability criterion. In Barmish and Shi [17] the case $m = 2$, $\mathbf{\Delta}(s) = P_{11}(s)P_{12}(s)+P_{21}(s)P_{22}$, was treated and alternative necessary and sufficient conditions for robust stability were derived. Kraus, Mansour and Anderson [154] showed that testing for real unstable roots of a multilinear polynomial could be achieved by examining the stability of a finite number of vertex polynomials while checking for unstable complex roots in general involved examining the real solutions of a set of simultaneous polynomial equations. In Zeheb [246] explicit necessary and sufficient conditions are derived for the case of two parameters. The representation given in Section 11.7 including Examples 11.6 and 11.7 are due to Dahleh, Tesi and Vicino [72] and the result described in Exercise 11.9 is due to Dahleh, Tesi and Vicino [70].